Final Report – Bonanza Spring: Assessing Source, Connections, Flow, and Vulnerabilities

September 2023

Sponsored by the Engineering Contractors' Association

Dr. Dave Kreamer, Principal Investigator
dave.kreamer@unlv.edu
(702) 895-3553
(702) 306-7107

Luke Stevens, Principal Scientist
luke.stevens@unlv.edu

Department of Geoscience
University of Nevada, Las Vegas
4505 Maryland Parkway, Box 454010
Las Vegas, NV 89154-4010

Bonanza Spring Report

Contents

List of Figures

List of Tables

Executive Summary

The purpose of this report is to provide insight into factors that might influence the long-term sustainability of Bonanza Spring, the largest spring in the Eastern Mojave Desert. To do this, a primary focus of this report is the potential relationship and connectivity between Bonanza Spring water and the possible sources of its flow. Methodologies included sampling of the spring, and well water south of the Clipper Mountains, California. This report presents the data collected during the 2022-2023 University of Nevada, Las Vegas (UNLV) Bonanza Spring Sustainability Study and provides analysis of the trace metal concentrations, major ion composition, and stable isotopes of Bonanza Spring and wells in, and surrounding, the Cadiz agricultural are located over 22 km to the southwest of the spring in the Bristol/Cadiz Basin. These represent the closest group of wells near the spring. Between 2022 and 2023, researchers from UNLV conducted over a year of sampling Bonanza Spring and surrounding wells in the Eastern Mojave Desert. This involved evaluation of aqueous physical properties, chemical characteristics, and related biological attributes. Sampling was monthly over the course of a year, along with a 24-hour round the clock sampling event. Raw data is presented in tables at the end of the report.

Review of past satellite imagery revealed both seasonal and annual temporal changes in the vegetation surrounding the spring. Aqueous water chemistry was analyzed by Inductively Coupled Mass Spectrometry (ICP-MS), supported by measurement of physical and chemical properties in the field. Principal Component Analysis (PCA) of trace water chemistry data revealed chemical differences and separation between the waters of Bonanza Spring and Cadiz wells for all three Principal Components considered. Water quality at the spring contains arsenic concentrations above EPA drinking water standards, as does well 35 when sampled in December. Aqueous concentrations of major ions of spring and well water were dissimilar, particularly considering percentages of divalent and monovalent cations. Stable isotope samples revealed differences in spring water versus well water. Additionally, comparison of stable isotope samples with rainfall showed spring water to be isotopically lighter than historical values of isotopes in local precipitation. Light stable isotope ratios of oxygen and hydrogen can be associated with precipitation at higher altitudes. Because the precipitation measurements were made just above the spring and the Clipper Mountains rise several hundred meters higher to the north, one possible interpretation would be that groundwater recharge supporting the spring's discharge originates from higher elevations in the Clipper Mountains and not at lower elevations in the lower Fenner Watershed or Bristol/Cadiz Basin. Previous analysis of faulting and fracturing in the Clipper Mountains supports this interpretation. No significant correlation was determined between antecedent rainfall events and water quality. Multiple lines of evidence discussed in this report suggest that Bonanza Spring and the wells in the Cadiz area of the Bristol/Cadiz Basin do not have a subsurface connection or common source.

The March 2023 sampling trip at the very end of the study followed a period of intense storms during a wetter than average winter that appear to have precipitated a flash flood, collapsing the tunnel at the spring orifice, damming the spring with clasts larger than six inches in diameter, preventing discharge from its previous point of issuance, and appearing to cause dieback of reeds. This change is evidence that several natural factors may episodically impact vegetative alteration and habitat availability in the spring environment.

Introduction

Springs are one of the most vital parts of a desert ecosystem and an essential element in Native American cultural traditions and heritage. In 2022, the University of Nevada, Las Vegas undertook research to better understand the history and sustainability of one of the largest springs in the Mojave Desert. Bonanza Spring is at latitude 34.69, longitude -115.41, approximately 18.9 kilometers northeast of Chambless, California in the eastern Mojave Desert (Figure 1). The spring is 640 meters above mean sea level or MAMSL (2100 ft above mean sea level or FASL), and is located on the southwestern flank of the Clipper Mountains which rise to 1,410 MAMSL (4625 FASL). The Clipper Mountains and Bonanza Spring are within the federally protected Mojave Trails National Monument under the administration of the U.S. Bureau of Land Management in San Bernardino County, California.

Many factors can affect the sustainability of springs. These include long-term climate change, geological changes that would impact hydraulic conductivity in the subsurface, changes in vegetation also taking account the influence of invasive species, and lowering of local piezometric surfaces due to groundwater extraction and nearby pumping wells. Considering the latter, there is some controversy as to whether pumping south of the Clipper Mountains near Cadiz could affect spring discharge at Bonanza. The Cadiz agricultural area is 22 kilometers (13.7 miles) to the south southwest of the spring, at approximately 240 MAMSL (785 FASL), with irrigation wells supporting the growth of crops in the Bristol/Cadiz Basin, California. The water table below Cadiz is located even lower in elevation below ground surface. It has been hypothesized that groundwater issuing from Bonanza Spring is hydraulically connected to the alluvial, basin-fill, Fenner Valley aquifer north of the Clipper Mountains, but also to lower Fenner Watershed to the south (Zdon et al. 2018). These authors put forward no reasonable explanation of what mechanism could cause groundwater in the lower Fenner Valley, or in the alluvial Bristol/Cadiz basin located more than 400 meters lower in elevation (>1,300 ft), to rise up to the higher level of Bonanza Spring to the north. Nor do they explain, if this undefined and hypothetical mechanism of groundwater rise were actually operative, why there aren't more springs located on the southern slopes of the Clipper Mountains with similar characteristics to Bonanza, all being fed by groundwater from hundreds of meters below to the south. One goal of this research was to investigate the similarity or dissimilarity of groundwater in Bonanza Spring versus Cadiz wells in the lower Fenner Watershed and Bristol/Cadiz Basin below and to the south, through a series of concurrent sampling and analysis of groundwater issuing from the spring and well water.

While this year-long study is insufficient time to assess transformations due to long-term changes including climate change, a collapse of the spring orifice during the study was observed to alter discharge characteristics and location, and subsequently a qualitative change in vegetation around the spring. Additionally, this study produced some supporting evidence for the nature of groundwater recharge characteristics for the spring that suggest future sustainability.

Literature and Satellite Imagery Review

As a beginning undertaking for this project, past reports, publications, and data were reviewed for previous studies on regional Mojave springs and wells, and the data compiled. A full list of initially reviewed articles is in Appendix A of this report. Geological and topographical review was conducted. Past Google imagery was also reviewed for an initial assessment of vegetative changes at Bonanza Spring and the Clipper Mountains. Figure 2 shows several selected Google Earth satellite images of Bonanza Spring at different past dates. Appendix B shows photographs from field locations around the spring.

Figure 1 Location of selected Cadiz production wells (blue points), monitoring wells (yellow points), and Bonanza Spring.

Figure 2. Example Google Earth satellite images of Bonanza Spring from 12/30/05, 2/19/07, 6/5/09, and 3/29/14, top image to bottom.

Analysis of Aerial Imagery

Aerial images from the National Agriculture Imagery Program (NAIP) were used to measure the extent of the riparian zone – the vegetated area around the spring supported by spring water – and to determine the Normalized Difference Vegetation Index (NDVI), a measurement of the difference between the brightness of the image using near infrared and red images. The NAIP dataset began in 2003 on a five-year cycle before switching to a three-year cycle in 2008. The images are collected by plane at a consistent altitude during the growing season. NAIP photography has data in four spectral bands, and data for Bonanza Spring is available for the years 2005, 2009, 2010, 2012, 2014, 2016, 2018, and 2020. All of the images are collected in spring or early summer, from April 25^{th} to June 30^{th}.

Figure 3 shows an example of an image resulting from NDVI analysis. The NDVI is derived according to the equation:

$$NDVI = \frac{NIR - Red}{NIR + Red}$$

The NDVI can vary between -1 and +1, with more positive values indicating the presence of vegetated areas and more negative values indicating standing water and other non-vegetated areas. Applying a Red-Green color ramp to the NDVI values creates an image that shows vegetation in green.

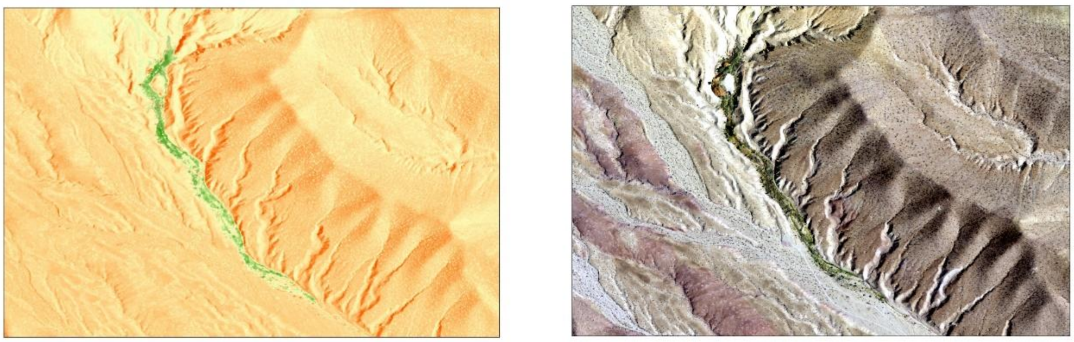

Figure 3. NDVI measured around Bonanza Spring and false color image. NAIP April 27, 2012.

NDVI allows one to identify the riparian zone more easily and can be used as a secondary indicator of spring health. Accurate measures of the riparian zone facilitate modelling of transpiration from the riparian vegetation, most notably the invasive reed *Arundo donax*. In addition to these analyses, two undergraduate workers underwent training in ArcGIS to continue analysis of aerial imagery datasets and to convert geologic maps and GPS gathered field information into shapefiles for future use. They are assessing the feasibility of tracking decadal *Arundo* prevalence using aerial images. Flora associated with the spring varied both seasonally and annually.

Weather and Climate Data

In addition to the rainfall totals above, the team compiled temperature and precipitation data from the nearest weather stations: Mid Hills, Ox Ranch, Amboy Saltus 1 and 2, Mitchell Caverns, the Clipper Mountains, and the Cadiz Valley. Precipitation data was available for all of these sites, and the table below summarizes the date range for relevant weather and climate parameters available for the sites. The Clipper Mountain weather data is derived from precipitation samplers that were checked twice yearly to measure winter and summer rainfall totals and the isotopic composition of these seasonal rains (Rose 2017). The Amboy Saltus 1 and 2 weather stations, operated from 1966-1989 and 1972-1993, have precipitation and temperature measurements that are included in our compiled dataset (Friedmann et al. 1992). The Amboy weather stations are separated by 50 m in elevation, which shows some precipitation totals varying with elevation in this part of the Mojave Desert.

Summary of Data Availability from Nearby Weather Stations					
Station	Latitude	Longitude	Precipitation Date Range	Temperature Date Range	Precipitation Isotopes
Amboy 1	34.53	-115.70	1966-1981	1972-1993	No
Amboy 2	34.48	-115.74	1972-1993	1972-1993	Yes
Cadiz Valley	34.52	-115.52	2011-Present	2011-Present	No
Clipper Mountans	36.69	-115.41	2001-2005	None	Yes
Mid Hills	34.56	-115.53	1958-Present	1958-Present	Yes
Mitchell Caverns	34.93	-115.51	1958-2011	1958-2011	Yes
Ox Ranch	35.20	-115.20	2013-2022	2013-2022	No

The Mojave Desert is generally considered Koppen Class BWk: hot in the summer and cool in the winter, similar to the Chihuahuan Desert. It has relatively cooler, higher desert elevations compared with the lower, warmer Sonoran Desert, and a different climate compared to other cold-temperate locations in the Great Basin. The nearest town to Bonanza Spring and Cadiz is Chambless CA, with the average summer high temperature at 36.7°C (98.1°F) occurring in July. In winter, the average high in December is 13.6°C (56.5°F) and the average low is 5.8°C (42.4°F). Like most dry desert climates the Mojave experiences large diurnal temperature changes. Annual rainfall in Chambless is 113 mm (4.45 in) over an average of 42.3 days (weather-us.com). Climate change has already increased temperatures in the region.

Rock Compositional Data

Compositional data of rocks from the Clipper Mountains were collected and reported by the USGS (Howard et al. 2005). This compositional data can relate to the analyses of water chemistry from Bonanza Spring and Cadiz wells by ICP-MS, as water flowing through these rocks could be compositionally similar. If water at Bonanza Spring is exclusively from the Clipper Mountain catchment, the water chemistry could be similar to rock compositions, after considering the mobility of elements and the oxides reported. Additional lithologic information from Cadiz wells or piezometers installed by Aquilogic could be useful for analyzing water samples for trace metals and could allow additional commentary on potential connections or lack of connection between Bonanza Spring and waters in the valley. For this study, only similarities or dissimilarities in aqueous concentrations will be addressed.

Correlation Analysis for Elemental Concentrations and Antecedent Rainfall

The influence of antecedent rainfall on water chemistry in Bonanza Spring can indicate long or short flow paths and the impact of surficial geology, with short flow paths being prevalent when samples show high variability following rainstorms. For this analysis, total rainfall data for a week and month prior to sampling from the Mid Hills weather stations in the Mojave National Preserve were used to compare to chemical concentrations in Bonanza Spring. The figures below show the concentrations of the most variable trace metals in the data set with the total rainfall for a week and month prior to sampling.

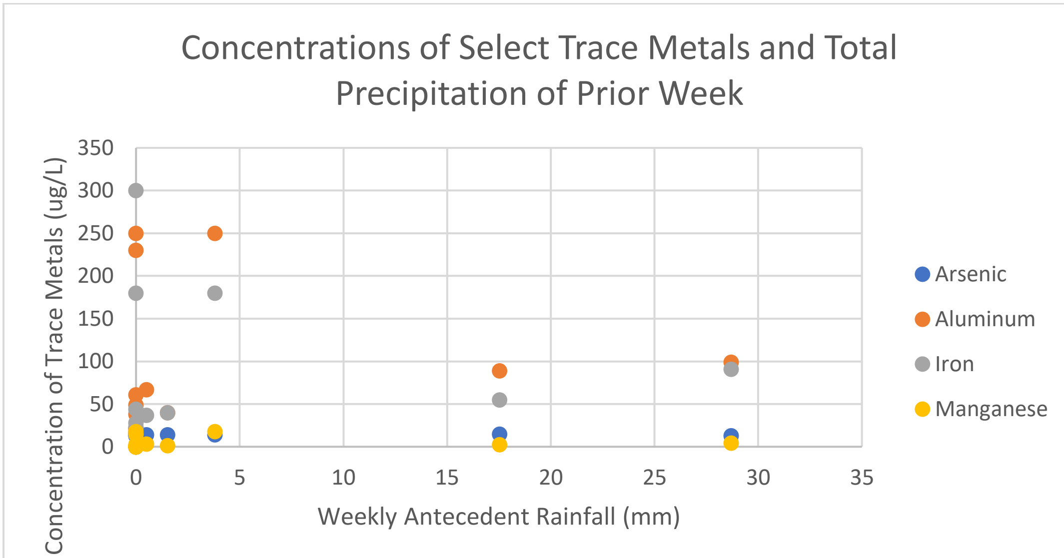

Figure 4. Concentrations of select trace metals in Bonanza Spring, dependent on total antecedent rainfall for the prior week.

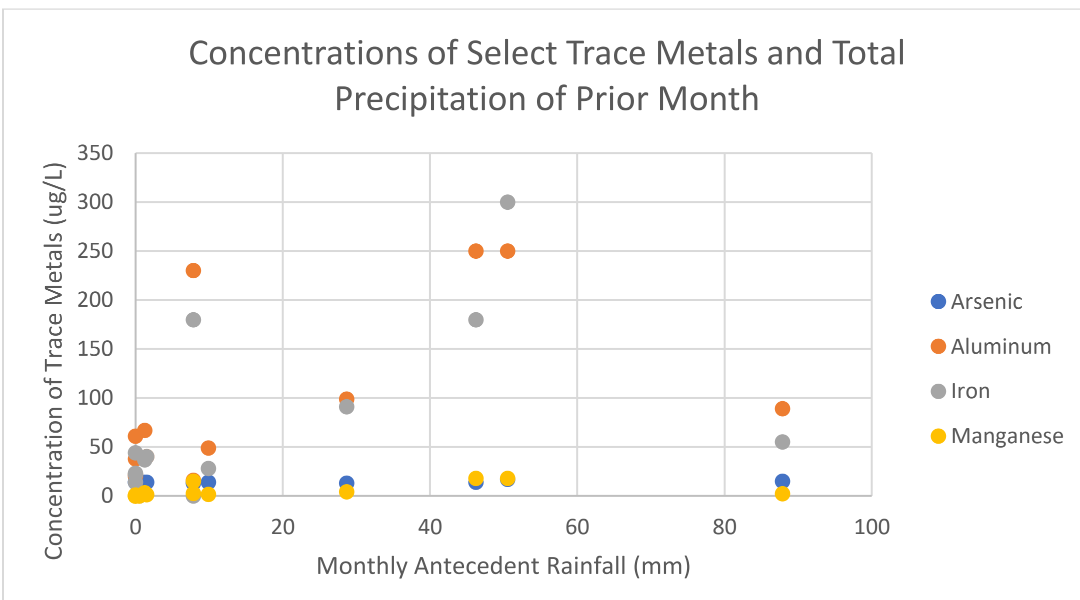

Figure 5. Concentrations of select trace metals in Bonanza Spring, dependent on total antecedent rainfall for the prior month.

There are no strong correlations ($R^2 > 0.50$), but the monthly antecedent rain data shows a slightly stronger positive correlation for aluminum and arsenic. This analysis used rainfall data from the Mid Hills weather station, the nearest for the sampling period (September 2018 – March 2022). Additional analysis of relations between antecedent rainfall and spring water chemistry will consider data from other nearby stations to provide a more accurate depiction of rainfall at Bonanza Spring.

Analysis of rainfall data in the Mojave Desert is complicated by the natural unpredictability and variability characteristic of all storms. The Mojave Desert shows different meteoric rainfall regions due to the different controls on regional precipitation. The Western Mojave tends to be drier due to stronger orographic effects, while the Southeastern Mojave tends to be wetter. The duration of rainfall can also impact this analysis, as sustained rainfall allows greater wetting of the soil and increased recharge to the subsurface.

Methodology and Results

Results of Trace Metal Sampling and Principal Component Analysis

Trace elements in groundwater can often be used to separate waters of like or dissimilar provenance. UNLV conducted sampling and analysis of aqueous samples to evaluate similarities or differences in the chemical makeup of waters south of the Clipper Mountains.

Methodology and Comparisons to EPA MCLs

Same-day water samples for trace elements were collected at both Bonanza Spring and Cadiz wells throughout 2022 and early 2023 according to EPA Method 1669. Samples were stored in acid-washed HDPE bottles using the clean and dirty hand method following collection in a syringe and filtration through a 45-micron filter in the field (US EPA, 2004). After collection, samples were stored on ice within 15 minutes and taken to the UNLV Las Vegas Isotope Science SEB 100 clean lab for acidification with nitric acid on the same day. Analysis was performed by the UNR Core Analytical Laboratory on a Shimadzu 2030 ICP-MS in Kinetic Energy Discrimination mode. This machine uses a hydride generator to remove interferences associated with the measurement of arsenic and antimony, two common contaminants of concern. Water quality at the wells with respect to metal concentrations was generally within drinking water limits established by the EPA. At Bonanza Spring, arsenic was consistently above the EPA MCL of 10 μg/L with an average concentration of 12.8 μg/L. Well 35 showed arsenic concentrations slightly above the MCL on January 28th, with the two samples averaging 10.53 μg/L (US EPA, 2007).

Introduction to Principal Component Analysis

Principal Component Analysis (PCA) is a multivariate statistical technique that uses dimension reduction to identify and group water samples that have comparable aqueous parameters. PCA can reduce data from n-variables to represent the ensemble of similar aqueous concentrations in a 2- or 3-dimensional plot. It can also identify dissolved aqueous compounds that are similar or dissimilar in different water samples (Kreamer et al., 1996). The axes of the plot are vectors that represent the greatest variability in the data. For this analysis, all parameters used were normalized and centered around 0 to prevent major ion constituents from dominating the variance. For elements or compounds in the data set with low concentration below the detection limits of analytical chemistry instruments, an alternative to reducing the data set is typically used. Synthetic, non-zero, low concentration data can be simulated, although the way a value for a non-detected compound is simulated varies based on concentrations for that compound in other groundwater sample locations in the complete data set (Farnham et al. 2002). The plots presented below used one of those techniques by assigning concentrations that are half the detection limit for compounds that were originally non-detects. This procedure simulates low aqueous concentrations, while allowing comparison through PCA analysis.

Analysis of Trace Metal Chemistry

For the PCA performed below, the parameters used were As, Ba, Ca, Ce, Dy, Er, Eu, Fe, Gd, Ho, K, La, Mg, Na, Nd, Pb, Pr, Sb, Se, Sm, Tb, Th, Tm, U, Yn, δD, and $\delta^{18}O$. The sites analyzed include Bonanza Spring, and Cadiz Wells 21N, 26, 27S, 33, and 35. Input parameters for the spring and well concentrations were the yearly average value for each individual element or parameter. This was done at each site for all measurements for each individual parameter, since strong seasonality was not observed. Analysis was completed using the R programming language's prcomp library, and ggplot was used for plotting (R Core Team, 2018).

Preceding PCA analysis, this method first normalized the data and centered it around 0, preventing major ions from dominating the variance and easing the graphical interpretation (Wilson et al., 2022). Covariance of each parameter with the other parameters was then determined, and a covariance matrix generated. Covariance denotes the degree to which two random variables in a data set will increase or decrease together at the same time, with positive covariance meaning they change in the same direction. This is not to be confused with correlation. In simple terms, both covariance and correlation measure the relationship and interdependence of two variables in different ways. Covariance specifies the directional trend of the linear relationship between variables with time (positive when both variables increase in aqueous concentration). On the other hand, correlation analysis quantifies both the directional trend, and includes the strength of the linear relationship between two paired variables with time.

The covariance matrix is shown in Figure 6 and compares paired parameters at the spring and wells. Figure 7 shows a covariance matrix computed for Bonanza Spring samples collected between October 2022 and January 2023. Cells in blue represent positive directional trends in aqueous concentration between paired elements while cells in red represent opposite trends. Strong directional relationships are seen between the paired lanthanides Eu, Er, Dy, Gd, Ho, Pr, Yb, and Tm. Other strong positive directional changes exist between As, Se, and U.

Principal Component Analysis was then performed. The first Principal Component accounted for 55.5% of the observed variance, and the second Principal Component accounted for 26.2% of the variance. The third Principal Component is also considered and represents 15.6% of the variance. These three components account for a cumulative 97.7% of the total variance in the dataset, suggesting that they sufficiently explain the observed chemistries. Table 1 (Appendix A) shows the percentage of total variance accounted for by each Principal Component. Relative weights of the parameters included in the Principal Components are shown in Table 2 (Appendix A), with larger magnitude values indicating a parameter that is significant to the Principal Component. K Means clustering was used to determine groupings of water sources. Our analysis suggested 4 cluster centers should be considered (Figure 8), however only cluster 1, containing wells 35, 21N and 27S, includes multiple sites (Figure 9). The separation between Bonanza Spring and the wells is preserved in all dimensions considered. The horizontal magnitude on the Principal Component plots is exaggerated so that equivalent vertical distances represent a smaller difference in chemistry. The clustered wells are expected due to their proximity to one another and their placement in the same aquifer.

The results of this PCA suggest that the waters at Bonanza Spring relative to the Cadiz wells are not connected. Additional monitoring of the wells and montane springs in the area could provide interesting insight into the hydrogeology of the system. Obvious end members to the aquifer exist at the Cadiz and Bristol dry lakes where the wells are regularly monitored, but trace metal chemistry data is sparse. PCA of these additional wells could provide further evidence against a connection between the lower Bristol/ Cadiz Basin alluvial aquifers and Bonanza Spring if the end members group with either Cluster 1 or the two independent wells or if they form a separate group.

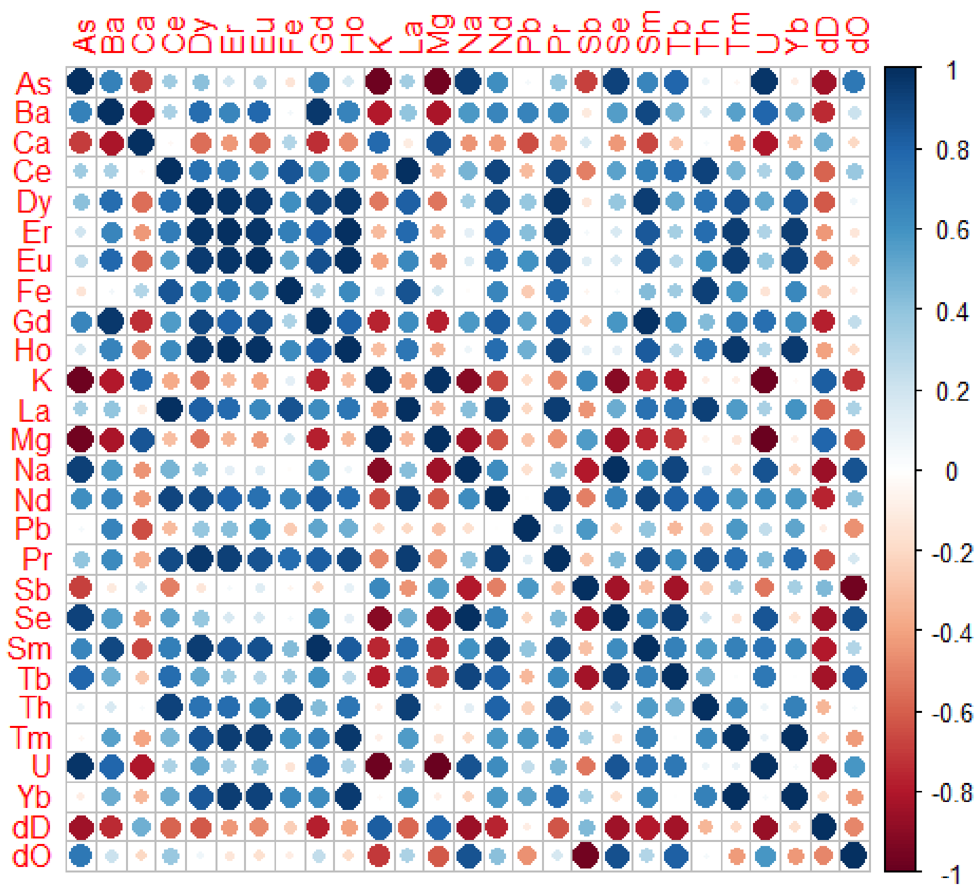

Figure 6. Covariance matrix used in the PCA. Compares parameters between the spring and wells. Intensity of Blue indicates positive covariance, that is the paired elements have similar directional increase or decrease in concentrations with time. Red intensity indicates paired elements have opposite directional changes in concentration with time.

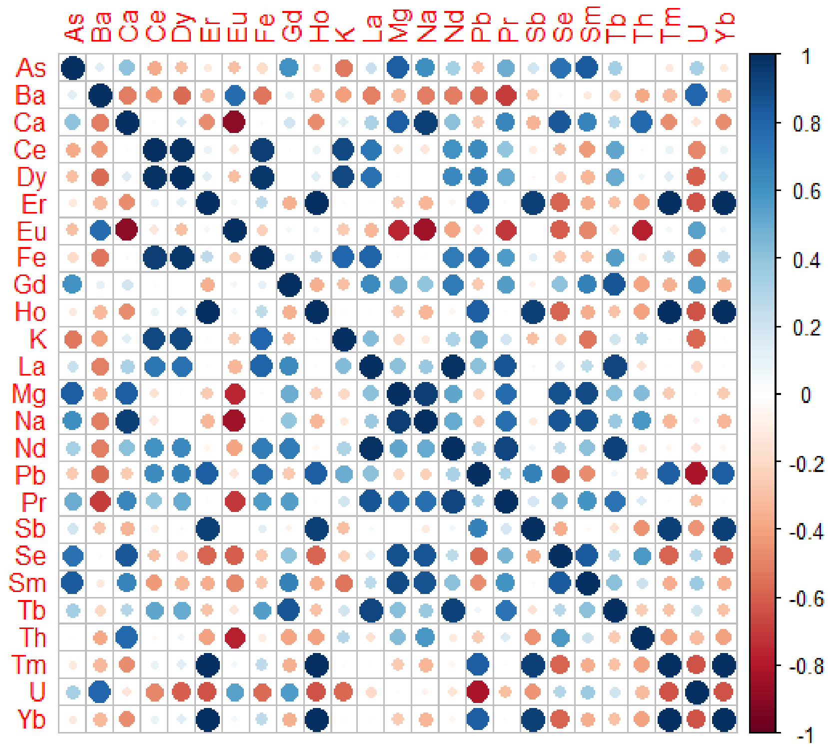

Figure 7. Covariance Matrix of Bonanza Spring Samples. Intensity of Blue indicates positive covariance, that is the paired elements have similar directional increase or decrease in concentrations with time. Red intensity indicates paired elements have opposite directional changes in concentration with time.

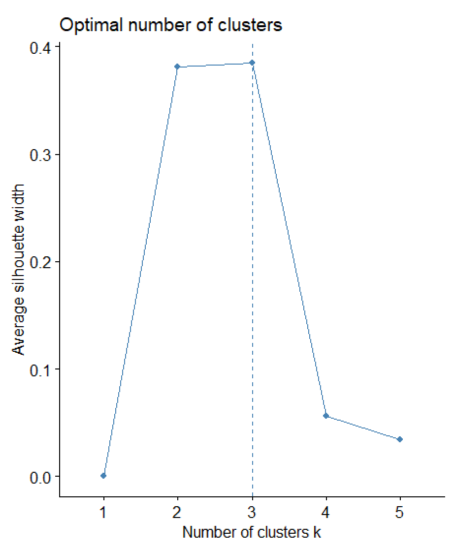

Figure 8. Optimal number of centers used in the K-means cluster analysis. The plot's knee, 4, is chosen.

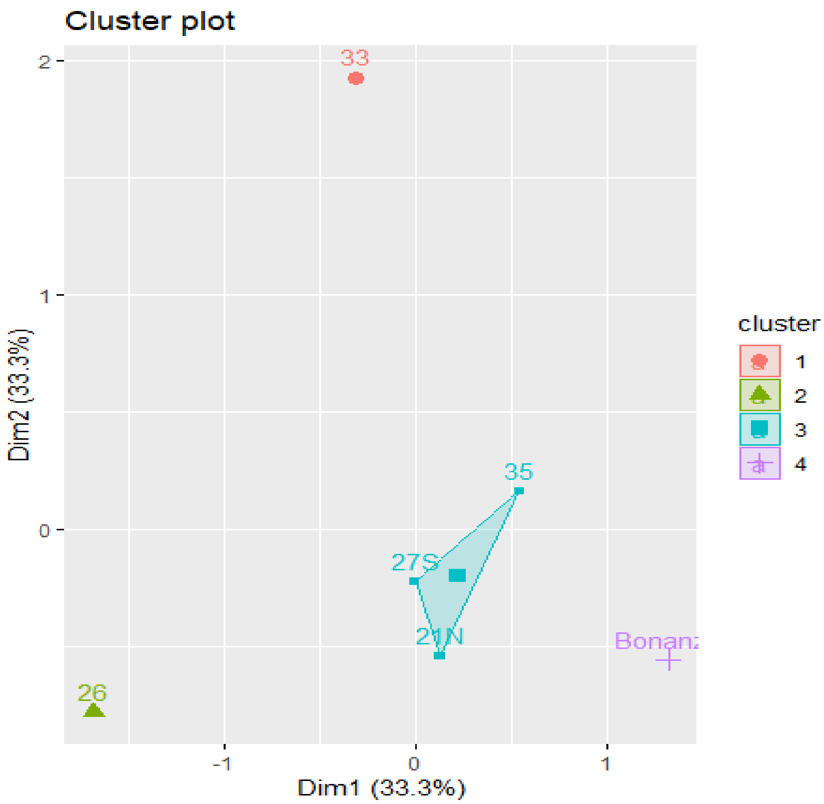

Figure 9. K-means cluster plot. Suggests at least 3 distinct groups, with Bonanza Spring having a dissimilar trace element signatures

The influence of individual elements in aqueous concentrations from the region can be addressed by considering the eigenvectors trace elements in a Principal Component Analysis plot of the waters. A biplot chemical elements of the first two Principal Components (PCs) is shown in Figure 10. The biplot shows significant separation between Bonanza Spring, and wells to the south in lower Fenner Watershed and Bristol/Cadiz Basins. The process is repeated for biplot of PCs 1 and 3 (Figure 11), and PCs 2 and 3 (Figure 12) with each showing considerable separation between Bonanza Spring and the sampled wells. Figure 13 is a 3-dimensional plot of the first 3 PCs. Again, Bonanza Spring stands apart in its aqueous chemical signature. This 3-dimensional plot is perhaps the best way to illustrate the significant water quality difference between Bonanza Spring and Cadiz wells, and is evidence to support the idea that these waters originate from different sources and flow pathways.

Though criteria vary, most PCA analyses project that if at least 70-80% of the total variance is explained by the first 4 or 5 Principal Components (PCs) the analysis is acceptable. If the variance is less than 60% the interpretation of results is more questionable. If, for example, the explained variance with the first few PCs is only 30%, the data is not considered useful and it may be necessary to revisit chemical analysis, and even the data collection process. As mentioned above and as shown in the scree plot in Figure 14, the first three PCs in this study explained 97.7% of the total variance in the data set, indicating a robust and acceptable analysis.

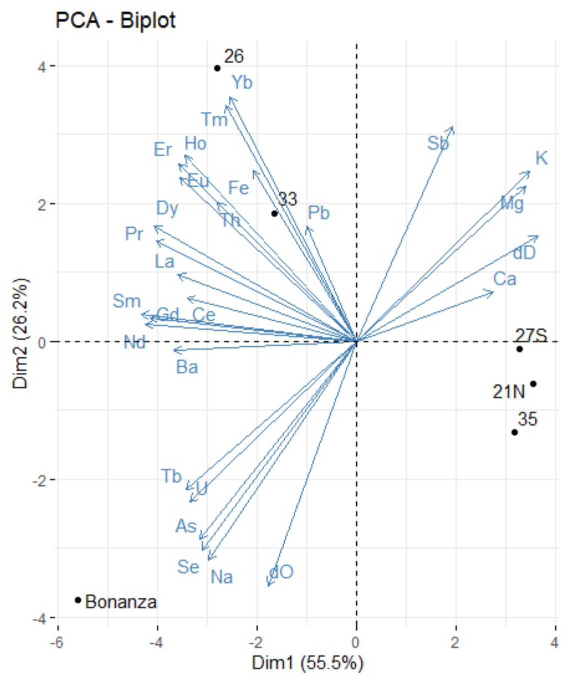

Figure 10. Principal Component plot with first two components. Eigenvectors shown in blue.

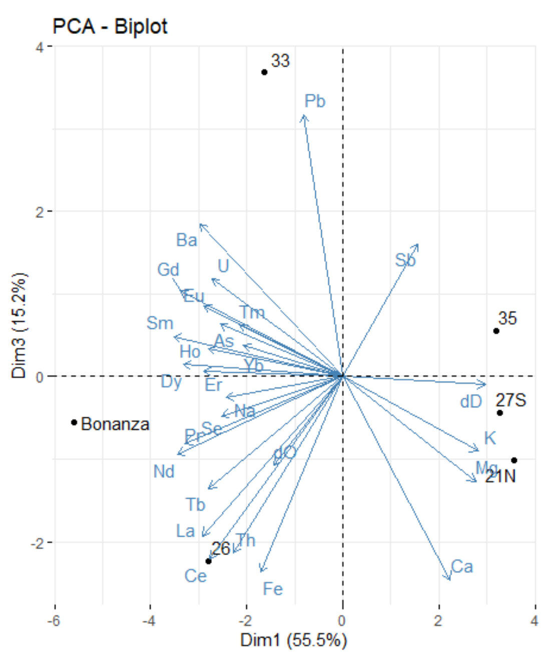

Figure 11. Principal Component plot using first and third PCs. Eigenvectors shown in blue.

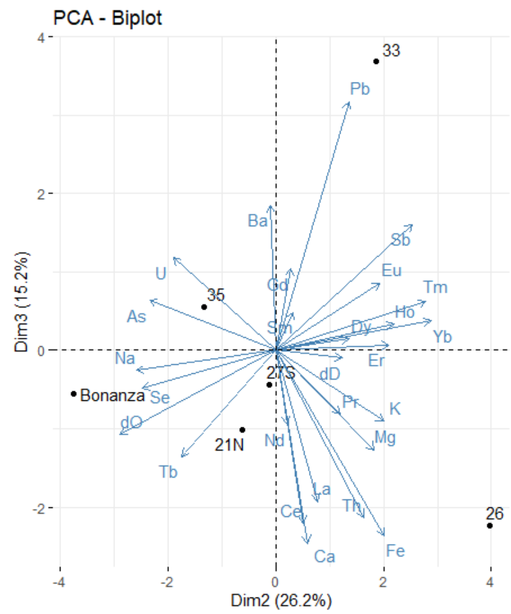

Figure 12. Principal Component plot using PCs 2 and 3. Eigenvectors shown in blue.

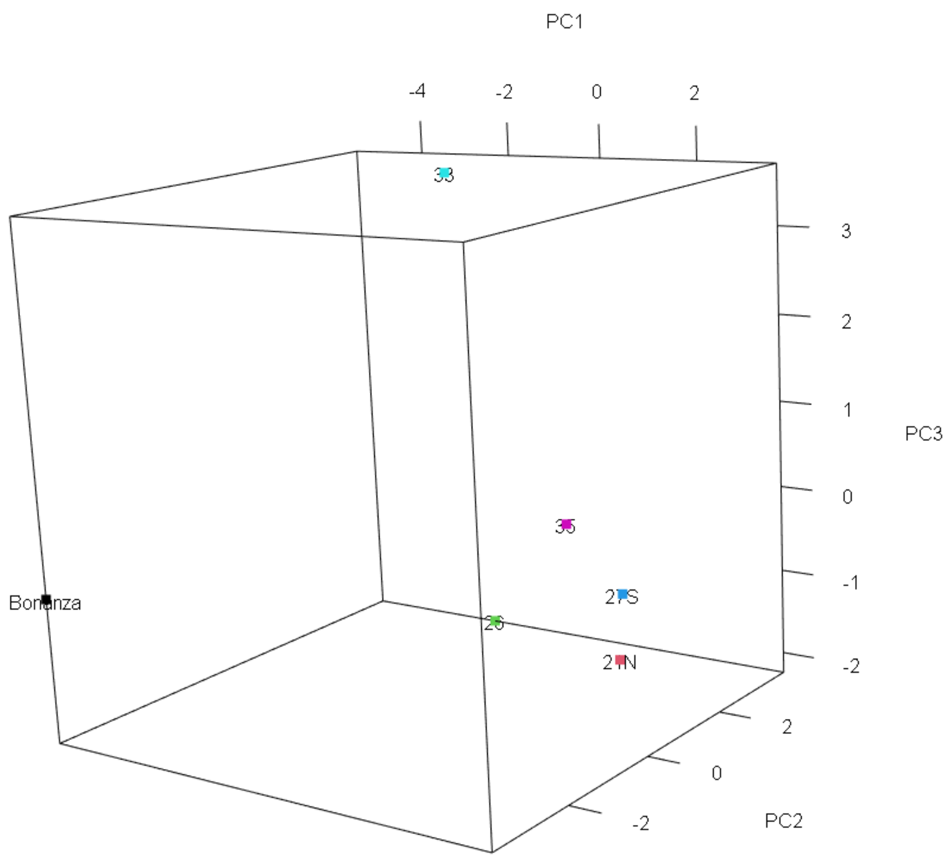

Figure 13. PCA represented in 3D. Wells 35, 27s, and 21N represent a distinct group.

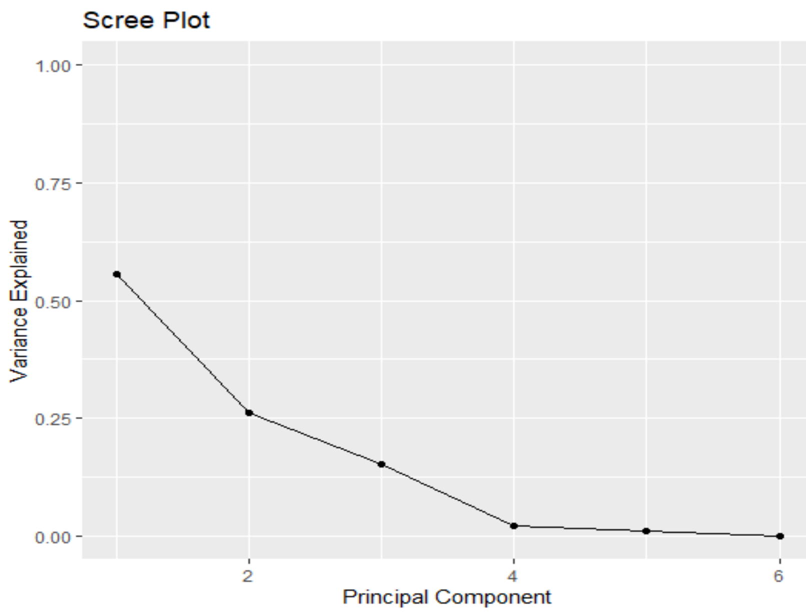

Figure 14. Scree Plot of variance explained by each Principal Component.

Major Ion Composition

Major ions include cations and anions that generally constitute the largest concentration elements in a water sample. Water types are often characterized by the largest of these constituents, and their concentrations can serve to identify the source aquifers of a sample. The water at Bonanza Spring and in the lower Fenner Watershed and Bristol/ Cadiz Basin is Na-HCO_3 type. Waters in the watersheds and basins below show the presence of calcium and magnesium which are found in much lower relative concentrations at Bonanza Spring, (approximately 20%).

Figure 15 shows the major ion chemistry of Bonanza Spring and wells 21N, 26, 27, 34, and 35 as measured by UNLV represented in a Piper diagram. The alluvium and carbonate points indicate averages for the lower Fenner Watershed and Bristol/ Cadiz Basin aquifers. Cation concentrations used in this plot come from analysis by ICP-MS. Analysis by ion chromatography (IC) results in higher values of calcium in all samples. Discussions with the lab managers suggest that the presence of sulfur in the samples could cause interference with calcium and inflate the measurement by IC, although using the ICP-MS results in a worse electric balance. Data from both measurements are presented in the appendices. Data presented in Figure 15 is from the ion chromatography analysis. This is because electric balances for those data indicated variation of less than 2%.

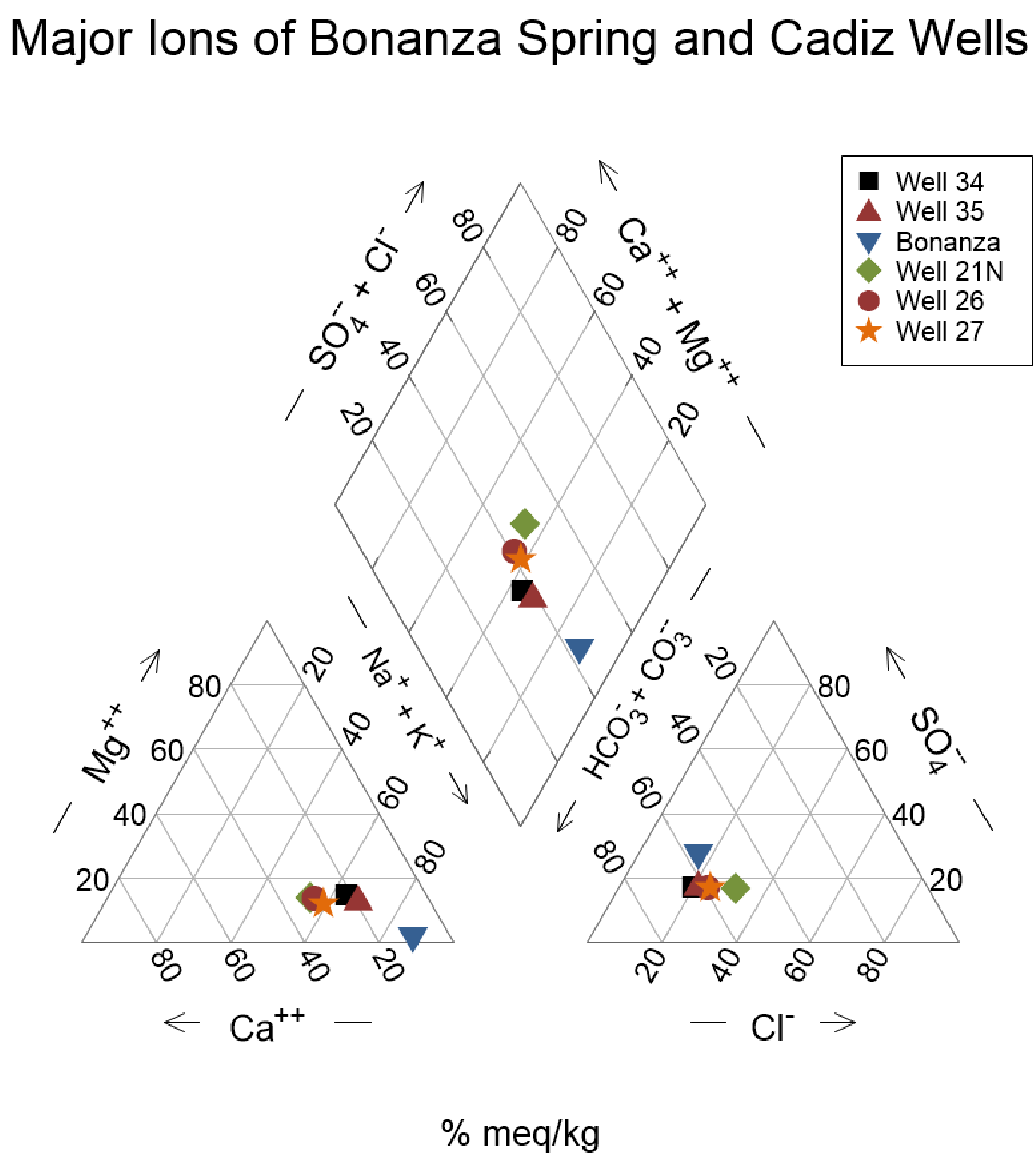

Figure 15. Piper diagram depicting the composition of the major ions in Bonanza Spring and wells in the wells in the Bristol/Cadiz Basin.

Hydrogen and Oxygen Isotope Analysis

Overview of Stable Isotopes

Stable isotopes were collected monthly for both Cadiz wells and Bonanza Spring. Isotope fractionation results from preferential evaporation of light isotopes, leaving behind the heavier isotopes of hydrogen and oxygen. These values are reported as a ratio of isotopic concentrations relative to a standard water, typically Standard Mean Ocean Water (SMOW). Elevation also influences isotopic values, with more light isotopes being found at high elevations. Temperature affects isotope values by contributing to evaporation, with cold weather resulting in lighter isotopic compositions than warm weather. In the basin and range province, winter precipitation generally dominates recharge (McGill 2020, Neff 2015). Stable isotopic measurements can help constrain recharge areas to groundwater systems and determine the water's origin. Average precipitation in the Mojave Desert averages between 3.5 and 10 inches annually, depending on elevation, with mountains receiving more precipitation.

The study period included historic monsoons and a wetter than average winter. These large rainstorms provide an opportunity to consider short flow paths to the spring orifice. The range of values for δD was 1.8‰ and 0.17‰ for $\delta^{18}O$. These isotopic values show very little change and great stability with time, providing evidence against rapid infiltration resulting in discharge at the spring. Figure 16 shows precipitation data collected by LLNL (Rose, 2017), well data collected by UNLV, and data collected at Bonanza Spring by UNLV and GSSI compared with the global meteoric water line (GMWL) and a local meteoric water line (Lachniet et al., 2020). The meteoric water line suggested in Lachniet et al. and the linear fit for the precipitation falling on the Clipper Mountains both show a slope lower than the GMWL, suggesting evaporation of samples occurred prior to collection. Figure 17 is an expanded view of a portion Figure 16 showing linear fits for both the wells, in orange, and Bonanza Spring, in grey and blue. The grey points represent data from the October 24 hour sampling period. There was no periodicity observed in the isotopic values, so variations during the period likely result from both temperature changes and random variations while sampling. Bonanza Spring consistently measures a lighter isotopic signature for δD, but $\delta^{18}O$ ratios generally measured heavier than the well waters. This could be a result of different ages of the water or presence of oxygen in aquifer materials. As water travels through an aquifer, water rock interactions can result in further fractionation of oxygen isotopes that would not result in changes to isotopic ratios of hydrogen.

A comparison of Bonanza Spring water stable isotopes measured in this study with precipitation isotopes measured by Lawrence Livermore National Laboratories, (LLNL) (Rose, 2017) was conducted. Figure 18 shows a satellite image of the location of the LLNL precipitation sampler north of Bonanza Spring about 350 m (1,150 ft) away and at an elevation of approximately 730 MAMSL (2,400 FASL), or about 90 m (300 ft) higher than the spring orifice. The average recharge from winter and summer precipitation for Bonanza Spring was quantified by LLNL using a simple linear mixing model for δ18O. The same analysis using δD was not possible due to Bonanza Spring having lighter isotopic ratios than measured by LLNL during both the winter and summer months. This analysis resulted in an estimated contribution of between 95% and 98% from winter precipitation to Bonanza Spring discharge, that is, the light winter rainfall isotopes dominated the comparable light isotopic signature at Bonanza Spring.

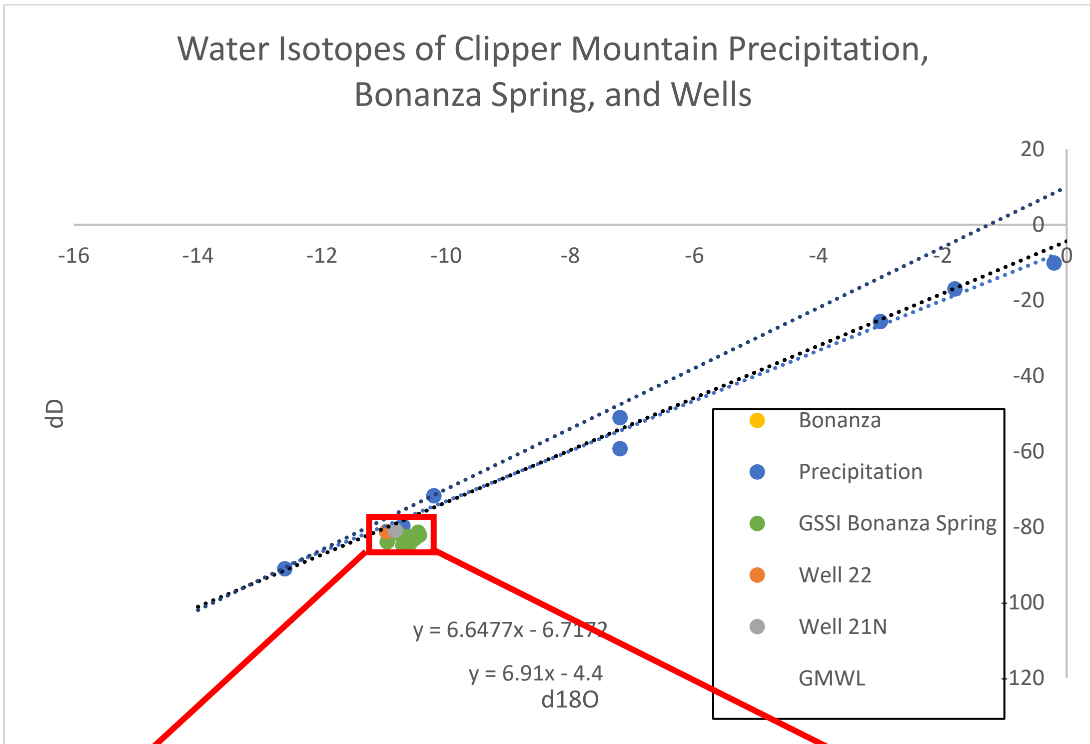

Figure 16. Stable isotopes of water. Blue points show precipitation isotopes measured by LLNL on the ridge above Bonanza Spring.

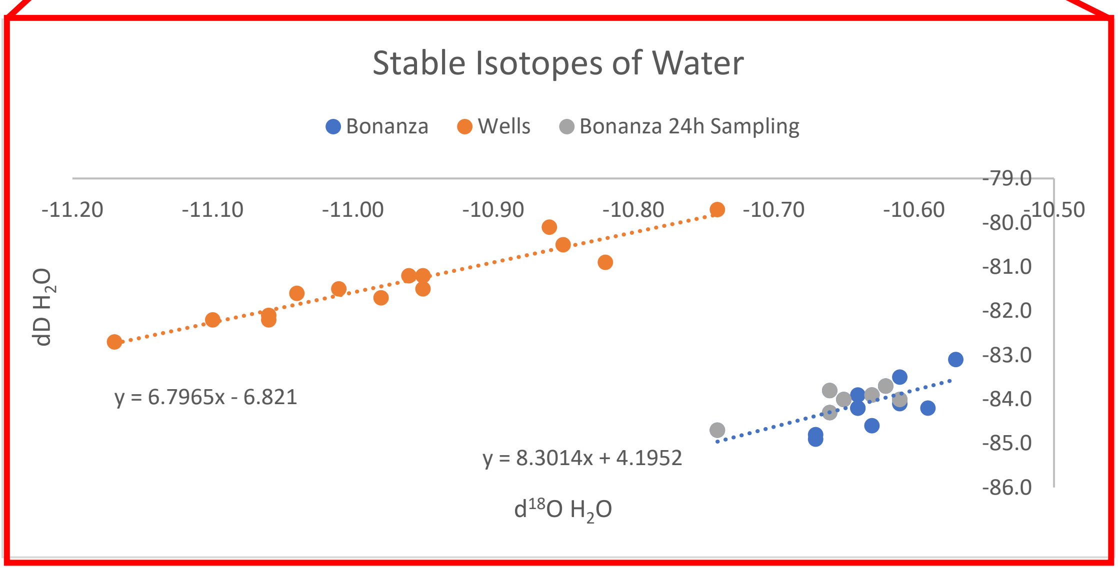

Figure 17. Expanded view - Stable Isotopes of Water - Bonanza spring and Fenner Valley Wells.

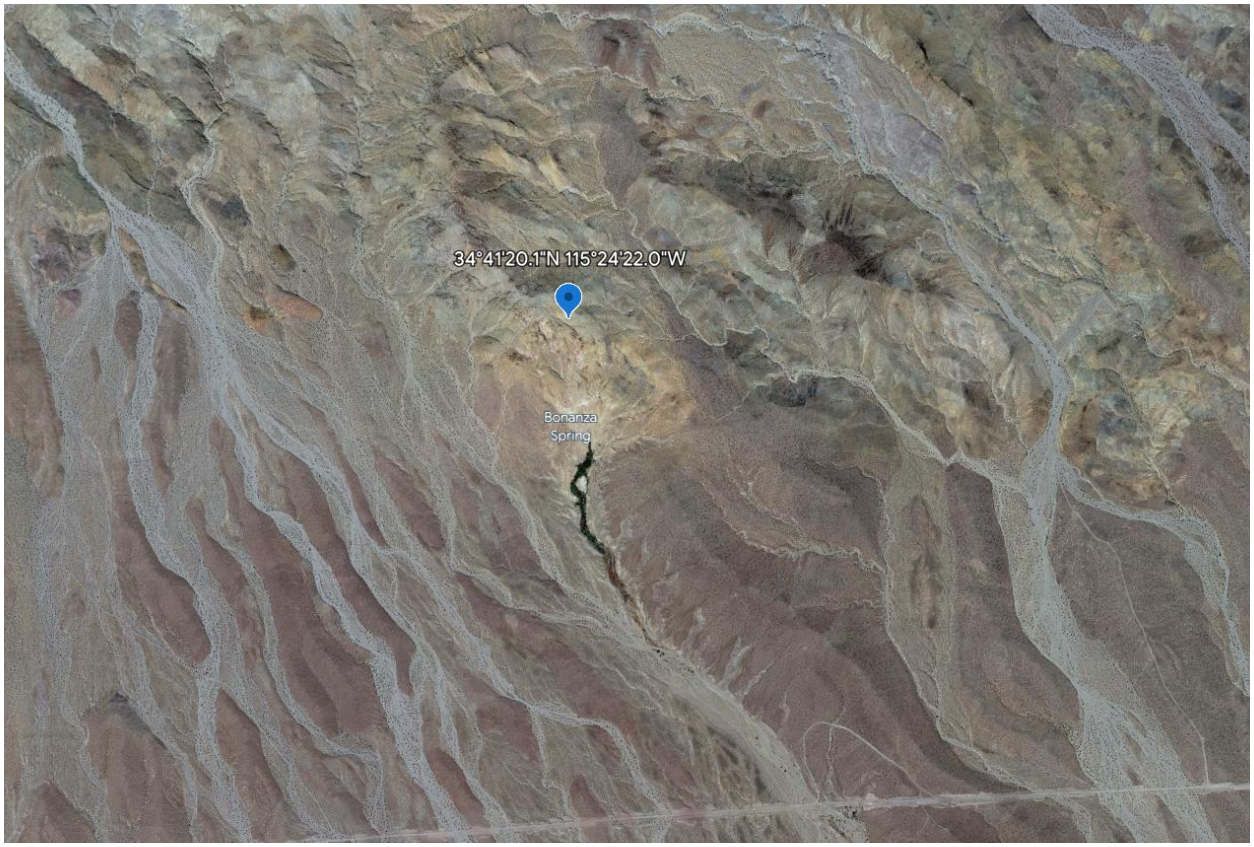

Figure 18. Satellite image of the location of LLNL precipitation sampler. The distance from the spring orifice to the sample is approximately 350 m (1,150 ft)

There are other possible explanations for these data differences between the range of LLNL rainfall isotopic values and the lighter, more consistent values at Bonanza Spring. This, for example, could be a result of evaporation of precipitation samples before collection by LLNL staff. Alternatively, recharge could occur at a higher elevation than the sampler was placed, such as in the higher ranges to the northwest of the spring. These immediately higher ridges reach elevations in the range of 150 m (500 ft) higher than the LLNL sampler and have been proposed as a recharge area by Aquilogic and Kenney Geosciences. The highest elevations considered within the recharge area by Aquilogic Inc. are approximately (1600ft) 487m higher than the placement of the LLNL precipitation gage. The Clipper Mountains north of the spring and LLNL precipitation measurement site rise an additional 680 m (2225 ft) above the LLNL site and would likely result in even lighter isotopic rainfall values.

Higher elevations generally receive lighter precipitation isotopes. Friedman et al. (2002) studied the impact of elevation changes on precipitation isotopes by analyzing the linear regression between weather stations separated by more than 400m within 50km of each other. This resulted in a slope between -5‰ and -10‰ per km for δD. Taking a weighted average of deuterium measured by the LLNL precipitation gauge, placed at an elevation of approximately 730 MAMSL (2,400 FASL), at the crest immediately above Bonanza Spring results in an average of -77.4‰, compared with a lighter average at Bonanza Spring of -84.1‰. While this LLNL data suggests the precipitation isotopes falling on the Clipper Mountains are still heavier than those found discharging at Bonanza Spring, Figure 16 shows that the slope of the precipitation measured by LLNL falls below the global meteoric water line, suggesting some evaporation has occurred that would artificially enrich the heavy isotopes. For further investigation, multiple precipitation stations in the Clipper Mountains could be used to construct an elevation-isotope regression for the mountain alone, although this would require many years of data due to the limitations discussed above. These would allow more precise determination of the isotopes of the precipitation falling on the Clipper Mountains and test the idea that high elevation precipitation falling locally provides sufficiently light isotopes to account for discharge at Bonanza Spring.

Another potential explanation for the data differences between the range of LLNL rainfall isotopic values and the lighter, more consistent values at Bonanza Spring could be the small size of the LLNL data set. Only 5 summer and 4 winter precipitation measurements were made, so individual precipitation events could vary greatly and thus bias the overall interpretation of the data. Future work quantifying evapotranspiration and precipitation at the site would need a long-term monitoring plan with multiple precipitation stations. Annual precipitation increases with elevation, so any samplers placed on these higher ridges would be expected to collect greater total rainfall. The higher elevation would also likely result in a lighter isotopic composition.

Additional isotopic samples were taken below the densely vegetated portion of the Bonanza Spring wash next to the rattlesnake information sign, referred to in some references as Lower Bonanza Spring. These samples are referred to as Alluvial, Below Rattlesnake Sign, and Rattlesnake Sign. Water use by plants, which preferentially uptake lighter isotopes, and evaporation contribute to a heavier isotopic signature downgradient. Figure 19 shows the results of these samples in blue. Of note is that the wash appears to be controlled by recent precipitation and evapotranspiration, drying up during the summer and flowing following precipitation events or when the temperature is cool enough to allow water emerging at Bonanza Spring to flow further. This is not seen at the spring orifice where water temperatures were measured with a range of 27ºC in February to 30.1ºC in October. The high stability of temperatures and low variations in stable isotope composition suggests that rapid flow paths do not influence the spring and baseflow is controlled by matrix flow through micropores. While Zdon et al. 2018 suggests the overlying volcanic material has permeability too low to allow infiltration, structural features, such as the fault trends, could provide areas of higher permeability that allow infiltration to depth and recharge the micropores micropores (Kenney and Foreman 2018). These fault trends, which Kenney and Foreman detail, consist of a conjugate fault system and two major faults that intersect at the spring. This fault system extends to the higher elevations of the Clipper Mountains and could be a recharge mechanism for isotopically lighter rainfall.

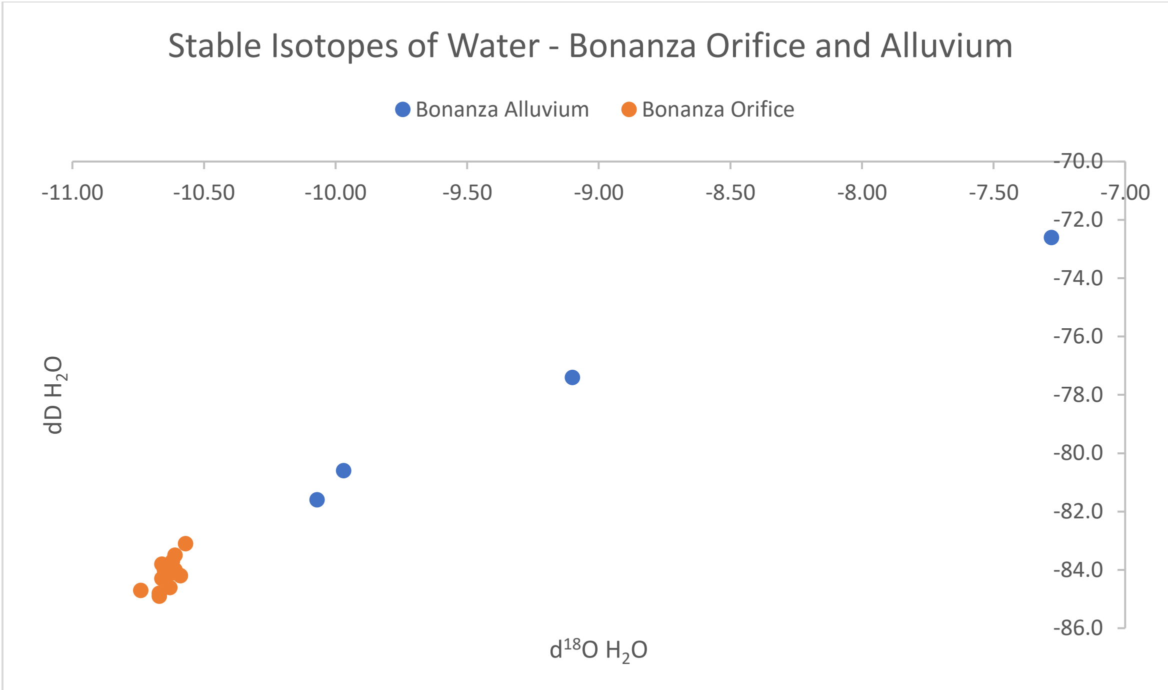

Figure 19. Stable Isotopes of Bonanza Spring Orifice and Bonanza Wash.

Changes in Spring Flow and Vegetation

March Spring Reconnaissance

Flood events, collapse features, and erosional geologic events can influence spring discharge. On March 25, 2023, during one of the UNLV research team's regular visits to Bonanza Spring, they found the tunnel at the spring orifice collapsed following an apparent flash flood. Large storms in California had been persistent in 2023. Previous reports showed the results of aerial image analysis for the NDVI of the spring's riparian zone. The NDVIs, a measure of plant photosynthetic greenness and an indicator of photosynthetic activity, showed that the riparian zone was active in early April 2012. The results of the image analysis for April 2012 are shown in Figure 3 on page 10 of this report. This image was chosen since it shows the driest soil surrounding the spring and therefore does not appear to be influenced by a recent precipitation event. Figure 20 shows the spring orifice dammed by clasts.

NDVI measures the difference between red and infrared light reflected by a plant. This value is then used to apply a color to each pixel, with greens suggesting photosynthetically active plants and red indicating water. The image in Figure 3 shows green pixels along much of the Bonanza wash. Figure 21 shows a picture taken on March 25, 2023 of the reeds at Bonanza Spring. A small patch of green reeds can be seen on the left side of the image, below some cottonwood trees. Of note is that the more deeply rooted cottonwood trees appear healthy while the *Arundo donax* reeds present on the right and center of the image appear wilted. These reeds are invasive and a potential major source of transpiration from the spring system. Previous efforts to remove them from riparian environments have proved unsuccessful due to the longevity of their seeds and rapid maturation (Bell 1997).

Figure 20. Bonanza Spring orifice, March 25, 2023.

Figure 21. Bonanza Spring reeds and cottonwood.

As of April 29, 2023 the spring orifice was still dammed. This has resulted in the disappearance of the pool of water that used to occur immediately below the orifice. Because of this, planned CFC and SF_6 sampling is unlikely to achieve the prolonged pumping rates necessary for these samples.

Summary

Between 2022 and 2023, the University of Nevada, Las Vegas conducted over a year of sampling Bonanza Spring and surrounding wells in the Eastern Mojave Desert. This involved evaluation of aqueous physical properties, chemical characteristics, and related biological attributes. Sampling was monthly over the course of a year, along with a 24-hour round the clock sampling event. Analysis of data revealed distinct differences between water quality attributes of spring and well water. Specifically, Principal Component Analysis of trace element concentrations in Bonanza Spring water versus wells in the Cadiz farming area to the south showed significant dissimilarities, as did major ion concentrations. Stable isotope samples revealed differences in spring water versus well water. Additionally, comparison of stable isotope samples showed spring water to be isotopically lighter than historical values of isotopes in local precipitation, suggesting a higher altitude recharge source for the spring than its immediate small watershed, including the possibility of recharge higher up in the Clipper Mountains above Bonanza Spring, and groundwater movement through higher fractured hard rock to its spring discharge point.

Alterations in the spring orifice and point of groundwater issuance changed dramatically late in the study in 2023, resulting in observable changes to the discharge amount, location, and in the spring's vegetative community that is dependent on flow.

Acknowledgements

The authors would like to thank the principal sponsor of this research, the Engineering Contractors' Association (now merged into United Contractors), and to the co-sponsors and supporters including: the Building Industry Association of Southern California, the Construction Industry Coalition on Water Quality, the Inland Empire Economic Partnership, the International Union of Operating Engineers – Local 12, the Laborers' International Union of North America – Southern California District Council of Laborers, Rebuild SoCal Partnership, and the Secure Water Alliance. Also, we would like to express our gratitude to students who helped with logistical support for field efforts, particularly Colin Davidson, Sandra Joseph, and Tyler Andreas.

References for this Report

Aquilogic Inc., Brown, A., Wildermuth, M., Romero, D., & Parker, T. (2019) Report Of The Independent Peer Review Panel For The Groundwater Management, Monitoring, And Mitigation Plan (Gmmmp) For The Cadiz Valley Groundwater Conservation, Recovery And Storage Project San Bernardino County, California. Aquilogic Inc. Costa Mesa, CA.

Bell, G., 1997. Ecology and management of *Arundo donax*, and approaches to riparian habitat restoration in Southern California. In Brock, J. H., Wade, M., Pysek, P., and Green, D. (Eds.): Plant Invasions: Studies from North America and Europe. Blackhuys Publishers, Leiden, The Netherlands, pp. 103-113.

Davisson, M. L., Smith, D. K., Kenneally, J., & Rose, T. P. 1999. Isotope hydrology of southern Nevada groundwater: Stable isotopes and radiocarbon. *Water Resources Research*, *35*(1), 279–294. https://doi.org/10.1029/1998WR900040

Farnham et al., 2002, Treatment of nondetects in multivariate analysis of groundwater geochemistry data, Chemometrics and Intelligent Laboratory Systems, 60, 265-281

Friedman, I., Harris, J.M., Smith, G.I., Johnson, C.A., 2002, Stable isotope composition of waters in the Great Basin, United States 1. Air-mass trajectories, Journal of Geophysical Research, 107: 14, DOI: 10.1029/2001JD000565

Kenney, M.D. and T.L. Foreman, 2018. Updated Assessment of Cadiz Water Project's Potential Impacts to Bonanza Springs. Report from Kenney Geoscience, Oceanside, CA and TLF Consulting, LLC, Camarillo, CA for Cadiz, Inc. January 2018.

Johannesson, K.H., Stetzenbach K. J. Hodge, V.F., Kreamer, D. K., & X. Zhou, 1997. Delineation of Ground-Water Flow Systems in the Southern Great Basin Using Aqueous Rare Earth Element Distributions. *Ground Water* Vol. 35, No. 5, p. 807-819.

Johannessonn, K.H., Stetzenbach, K.J., Kreamer, D.K., and V.F. Hodge, 1996. Multivariate Statistical Analysis of Arsenic and Selenium Concentrations in Groundwaters from South-Central Nevada and Death Valley, California. *J. of Hydrology*. Vol.178, 1-4, pp.181-204.

Kreamer, D. K., Hodge, V. F., Rabinowits, I., Johannesson, K. H., & Stezenbach, K. J., 1996. Trace Element Geochemistry in Water from Selected Springs in Death Valley National Park, California. *Ground Water*, *34*(1), 94–103.

Lachniet, M. S., Asmerom, Y., Polyak, V., & Denniston, R. 2020, Great Basin paleoclimate and aridity linked to Arctic warming and tropical Pacific Sea surface temperatures. Paleoceanography and Paleoclimatology, 35, e2019PA003785. DOI: 10.1029/2019PA003785

Neff, K.L., 2015, Seasonality of groundwater recharge in the basin and range province, western North America, Dissertation, the University of Arizona University Libraries, 10150/556969

R Core Team, 2018. R: A language and environment for statistical computing. R Foundation forStatistical Computing, Vienna, Austria. URL https://www.R-project.org/.

Rose, T.P., 2017, Data measured on water collected from eastern Mojave desert, California: Lawrence Livermore National Laboratory, LLNL-TR-737159, 10 p.

United States Environmental Protection Agency, 2007. *Arsenic in your drinking water*. EPA NEPIS. Retrieved March 29, 2023, from https://nepis.epa.gov/Exe/ZyPDF.cgi?Dockey=60000E1E.txt

U.S.EPA REGION 9 LABORATORY, 2004. *Trace metal clean sampling of Natural Waters*. Retrieved March 24, 2023, from https://ndep.nv.gov/uploads/env-brownfields-qaplans-docs/SOP_Trace_Metal_Clean_Sampling_of_Natural_Waters_R9.pdf

Wilson, J.W., Erhardt, A.E, & Tobin, B.W., 2022, Isotopic and geochemical tracers of groundwater flow in the Shivwits Plateau, Grand Canyon National Park, USA, Hydrogeology Journal, 30:495-510, DOI: 10.1007/s10040-022-02450-3

Zdon, A., Davisson, M.L. and A. H. Love (2018) Understanding the source of water for selected springs within Mojave Trails National Monument, California, Environmental Forensics, 19:2, 99-111, DOI: 10.1080/15275922.2018.144890

Appendix A: Initially Reviewed Literature for this Project/ Bibliography

Andy Zdon and Associates, Inc. 2016. Mojave Desert Springs and Waterholes: Results of the 2015–16 Mojave Desert Spring Survey, Inyo, Kern, San Bernardino and Los Angeles Counties, California. Prepared for Transition Habitat Conservancy and U.S. Bureau of Land Management. November 11. Arnold J. R. and Libby W. F. (1949) Age determinations by radiocarbon content: checks with samples of known age. Science 110, 678–680

Asante, J., Dotson,S., Hart, E. and D.K. Kreamer 2018. *Water Circulation in Karst Systems: Comparing Physicochemical and Environmental Isotopic Data Interpretation.* Environmental Earth Sciences, 77:421. Springer Nature.

Asante, J. and D. K. Kreamer, 2018. *Identifying local and regional groundwater in basins: chemical and stable isotopic attributes of multivariate classification of hydrochemical data, the Lower Virgin River Basin, Nevada, Arizona and Utah, U.S.A,* Isotopes in Environmental and Health Studies, 54(4):370-391. DOI: 10.1080/10256016.2018.1444611.

Asante, J. and D.K. Kreamer, 2015. *A New Approach to Identify Recharge Areas in the Lower Virgin River Basin and Surrounding Basins by Multivariate Statistics*. Mathematical Geosciences, Published Online: 12 February 2015 DOI 10.1007/s11004-015-9583-0

Belcher, W.R., Sweetkind, D.S., Faunt, C.C., Pavelko, M.T., and Hill, M.C., 2017, An update of the Death Valley regional groundwater flow system transient model, Nevada and California: U.S. Geological Survey Scientific Investigations Report 2016-5150, 74 p., 1 pl. https://doi.org/10.3133/sir20165150 ISSN: 2328-0328 (online)

Busenberg E. and Plummer L.N. (1992) Use of chlorofluorocarbons (CCl3F and CCl2F2) as hydrologic tracers and age-dating tools: The alluvium and terrace system of Central Oklahoma. *Water Resour. Res.***28(9)**, 2257-2283.

Busenberg E., Weeks E.P., Plummer L.N. and Bartholemay R.C. (1993) Age dating ground water by use of chlorofluorocarbons (CCl3F and CCl2F2), and distribution of chlorofluorocarbons in the unsaturated zone, Snake River Plain aquifer, Idaho National Engineering Laboratory, Idaho. *U.S. Geological Survey Water-Resources Investigations* **93-4054**, 47.

Chapelle, F., Landmeyers, J.E., and F. H. Chapelle. *The Hidden Sea: Ground Water, Springs, and Wells.*Tucson, AZ: Geoscience Press, 1997. CLARK, I.D., FRITZ, P., Environmental Isotopes in Hydrogeology, Springer Verlag, Berlin, Heidelberg, New York (1997).

Clark, W.B., Jenkins, W.J., and Top, Z., 1976, Determination of tritium by mass spectrometric measurement of 3He: International Journal of Applied Radiation and Isotopes, v. 27, p. 515-522

Cook P.G. and Solomon D.K. (1995) The transport of atmospheric trace gases to the water table: Implications for groundwater dating with chlorofluorocarbons and Krypton-85. *Water Resour. Res.***31(2)**, 263-270.

Cook P.G. and Solomon D.K. (1997) Recent advances in dating young groundwater: chlorofluorocarbons, 3H/3He, and 85Kr. *J. Hydrol.* **191**, 245-265.

Cook P.G., Solomon D.K., Plummer L.N., Busenberg E. and Schiff S.L. (1995) Chlorofluorocarbons as tracers of groundwater transport processes in a shallow, silty sand aquifer. *Water Resour. Res.* **31(3)**, 425-434.

Cook P.G., Solomon D.K., Sanford W.E., Busenberg E., Plummer L.N. and Poreda R.J. (1996) Inferring shallow groundwater flow in saprolite and fractured rock using environmental tracers. *Water Resour. Res.* **32(6)**, 1501-1509.

Davisson, M. L., and Rose, T. P. 2000. Maxey–Eakin Methods for Estimating Groundwater Recharge in the Fenner Watershed, Southeastern, California. U.S. Department of Energy, Lawrence Livermore National Laboratory, UCRL-ID-139027. May 15. 7p.

Deines, P., Langmuir, D., Harmon, R.S., Stable carbon isotope ratios and the existence of a gas phase in the evolution of carbonate groundwaters, Geochim. Cosmochim. Acta 38 (1974) 1147–1164.

Drimmie, R.J., et al., Radiocarbon and stable isotopes in water and dissolved constituents, Milk River aquifer, Alberta, Canada, Appl. Geochem. 6 (1991) 381–392.

Dunkle, S.A., Plummer, L.N., Busenberg, E., Phillips, P.J., Denver, J.M., Hamilton, P.A., Michel, R.L., and Coplen, T.B., 1993, Chlorofluorocarbons (CCl3F and CCl2F2) as Dating Tools and Hydrologic Tracers in Shallow Ground Water of the Delmarva Peninsula, Atlantic Coastal Plain, United States: Water Resources Research, v. 29, no. 12, p. 3837-3860.

Ekwurzel B., Schlosser P., Smethie W.M., Jr., Plummer L.N., Busenberg E., Michel R.L., Weppernig, R. and Stute M. (1994) Dating of shallow groundwater: Comparison of the transient tracers 3H/3He, chlorofluorocarbons and 85Kr. *Water Resour. Res.* **30(6)**, 1693-1708.

Hach USA. *DREL Complete Water Quality Lab*. Hach. Retrieved March 24, 2022, from https://www.hach.com/drel-complete-water-quality-lab/product?id=20406211001#

Hendry, M.J., Wassenaar , L.I., Origin and migration of dissolved organic carbon fractions in a clay-rich aquitard: 14C and δ13C evidence, Water Resour. Res. 41 (2005) W02021.

Fontes, J.-C., Dating of groundwater, Guidebook on Nuclear Techniques in Hydrology, Tech. Rep. Ser. 91 (1983) 285–317.

Hanshaw B. B., Back W., and Rubin M. (1965) Radiocarbon determinations for estimating groundwater flow velocities in central Florida. *Science* 148, 494–495.

Harms, P.A. 2015. DISTRIBUTION OF TRITIUM IN PRECIPITATION AND SURFACE WATER IN CALIFORNIA. M.S. Thesis, California State University, East Bay.

Hayes J.M. and Thompson G.M. (1977) Trichlorofluoromethane in groundwater - A possible indicator of groundwater age. Water Resources Research Center, Technical Report 90, Purdue University, NTIS Report PB 265 170, 25p.

IAEA 2013. Isotope Methods for Dating Old Groundwater, International Atomic Energy Agency, Vienna. https://www-pub.iaea.org/MTCD/Publications/PDF/Pub1587_web.pdf

Ingraham, N., K. Zukosky, and D.K. Kreamer, 2001. The Application of Stable Isotopes to Identify Problems in Large-Scale Water Transfer in Grand Canyon National Park. *Environmental Science and Technology*, 35-7 (1299-1302).

Kreamer, D.K., Stevens, L.E., and J.D. Ledbetter, 2015. *Groundwater Dependent Ecosystems – Policy Challenges and Technical Solutions,* in "Groundwater, Hydrochemistry, Environmental Impacts and Management Impacts, Nova Publishers, New York. Chapter 9, in "Groundwater: Hydrochemistry, Environmental Impacts, and Management Practices", Segun Adelana, Ed. P. 205-230. ISBN 978-1-63321. Online Access: https://www.novapublishers.com/catalog/product_info.php?products_id=52986&osCsid=be410bfe49edb2ea0ea3239891d33244

Kreamer, D.K. and A.E. Springer, 2008. The Hydrology of Desert Springs in North America, *in Aridland Springs in North America, Ecology and Conservation,* eds. L.E. Stevens and V. J. Meretsky, University of Arizona Press, Tucson ISBN 978-0-8165-2645-1.

Kreamer, D.K., Stetzenbach, K.J., Hodge, V.F., Johanneson, K. and I. Rabinowitz, 1996. Trace Element Geochemistry in Water from Selected Springs in Death Valley National Park, California. *Ground Water.* 34-1, p.95-103 (Jan-Feb. 1996).

Kreamer, D.K., Weeks, E.P. and G.M. Thompson, 1988. A Field Technique to Measure the Tortuosity and Sorption-Affected Porosity for Gaseous Diffusion of Materials in the Unsaturated Zone with Experimental Results from near Barnwell, South Carolina. *Water Resources Research,* Vol. 24, No. 3, p.331-341.

Johannessonn, K.H., Stetzenbach K. J. Hodge, V.F., Kreamer, D. K. And X. Zhou, 1997. Delineation of Ground-Water Flow Systems in the Southern Great Basin Using Aqueous Rare Earth Element Distributions. *Ground Water* Vol. 35, No. 5, p. 807-819.

Johnston C.T., Cook P.G., Frape S.K., Plummer L.N., Busenberg E. and Blackport R.J. (1998) Ground water age and nitrate distribution within a glacial aquifer beneath a thick unsaturated zone. *Ground Water* **36(1)**, 171-180.

LaMoreaux, Philip E.; Tanner, Judy T, eds. (2001), *Springs and bottled water of the world: Ancient history, source, occurrence, quality and use*, Berlin, Heidelberg, New York: Springer-Verlag, *ISBN 3-540-61841-4.*

Libby W. F. (1946) Atmospheric helium three and radiocarbon from cosmic radiation. Phys. Rev. 69, 671–673

Long, A., Murphy, E.M., Davis, S.N., Kalin, R.M., "Natural radiocarbon in dissolved organic carbon in groundwater", Radiocarbon after Four Decades: An Interdisciplinary Perspective (1992) 288–308.

Manga, M. "Using Springs to Study Groundwater Flow and Active GeologicProcesses."*Annual Reviews of Earth and Planetary Sciences*29 (2001):203–230

Meinzer, M. O.*Large Springs in the United States.*U.S. Geological Survey, WaterSupply Paper 557 (1927) Munnich K. O. (1957) Messungen des 14C-Gehaltes vom hartem Grundwasser. *Naturwisschaften* 44, 32–33.

Murphy, E.M., Davis, S.N., Long, A., Donahue, D., Jull, A.J.T., 14C in fractions of dissolved organic carbon in groundwater, Nature 337 (1989) 153–155.

Murphy, E.M., Davis, S.N., Long, A., Donahue, D., Jull, A.J.T., Characterization and isotopic composition of organic and inorganic carbon in the Milk River aquifer, Water Resour. Res. 25 (1989) 1893–1905.

Neretnieks, I., Diffusion in the rock matrix: An important factor in radionuclide retardation, J. Geophys. Res. 85 (1980) 4379–4397.

Neretnieks, I., Age dating of groundwater in fissured rocks: Influence of water volume in micropores, Water Resour. Res. 17 (1981) 421–422.

Oster H., Sonntag C. and Munnich K.O. (1996) Groundwater age dating with chlorofluorocarbons. *Water Resour. Res.* **32(10)**, 2989-3001.

Pearson F. J. (1966) Ground-water ages and flow rates by the C14 method. PhD, University of Texas

Phillips, F.M., Castro, M.C., Groundwater dating and residence time measurements, Treatise on Geochemistry 5 (2003) 51–497.

Phillips, F.M., Tansey, M.K., Peeters, L.A., Cheng, S., Long, A., An isotopic investigation of groundwater in the central San Juan Basin, New Mexico: Carbon-14 dating as a basis for numerical flow modeling, Water Resour. Res. 25 (1989) 2259–2273

Plummer L.N., McConnell J.B., Busenberg E., Drenkard S., Schlosser P. and Michel R.L. (1998a) Flow of river water into a karstic limestone aquifer 1. Tracing the young fraction in groundwater mixtures in the Upper Floridan aquifer near Valdosta, Georgia. *Appl. Geochem.* 13(8), 995-1015.

Plummer L.N., Busenberg E., Drenkard S., Schlosser P., McConnell J.B., Michel R.L., Ekwurzel B. and Weppernig R. (1998b) Flow of river water into a karstic limestone aquifer 2. Dating the young fraction in groundwater mixtures in the Upper Floridan aquifer near Valdosta, Georgia. *Appl. Geochem.* 13(8), 1017-1043

Plummer L.N., Michel R.L., Thurman E.M. and Glynn P.D. (1993) Environmental tracers for age-dating young ground water. In *Regional Ground-Water Quality,* ed. W.M. Alley, pp. 255-294, Van Nostrand Reinhold, New York, N.Y

Purdy, C.B., Burr, G.S., Rubin, M., Helz, G.R., Mignerey, A.C., Dissolved organic and inorganic 14C concentrations and ages for Coastal Palin aquifers in southern Maryland, Radiocarbon 34 (1992) 654–663.

Randall J.H. and Schultz T.R. (1976) Chlorofluorocarbons as hydrologic tracers: A new technology. *Hydrology Water Resources Arizona Southwest* **6**, 189-195.

Randall J.H., Schultz T.R. and Davis S.N. (1977) Suitability of fluorocarbons as tracers in ground water resources evaluation. *Technical report to Office of Water Research and Technology, U.S. Department of the Interior*, NTIS PB 277 488, 37pp.

Reilly T.E., Plummer L.N., Phillips P.J. and Busenberg E. (1994) The use of simulation and multiple environmental tracers to quantify groundwater flow in a shallow aquifer. *Water Resour. Res.* **30(2)**, 421-433.

Rose, T. P. 2017. Data Measured on Water Collected from Eastern Mojave Desert, California.

Lawrence Livermore National Laboratory, LLNL-TR-737159. August 18.

Sanford, W.E., Correcting for diffusion in carbon-14 dating of groundwater, Groundwater 35 (1997) 357–361.

Scanlon, B.R., Healy, R.W., Cook, P.G., Choosing appropriate techniques for quantifying groundwater recharge, Hydrogeol. J. 10 (2002) 18–39.
Schultz T.R. (1979) *Trichlorofluoromethane as a ground-water tracer for finite-state models*. Ph.D. Dissertation, University of Arizona.
Schultz T.R., Randall J.H., Wilson L.G. and Davis S.N. (1976) Tracing sewage effluent recharge- Tucson, Arizona. *Ground Water* **14**, 463-470.
Stewart, G. L., & Farnsworth, R. K. (1968). United States Tritium Rainout and Its
Hydrologic Implications. *Water Resources Research*, 4(2), 273–289.
Sudicky, E.A., Frind, E.O., Contaminant transport in fractured porous media: Analytical solutions for a system of parallel fractures, Water Resour. Res. 18 (1982) 1634–1642.
Sudicky, E.A., Frind, E.O., Contaminant transport in fractured porous media: Analytical solution for a two-member decay chain in a single fracture, Water Resour. Res. 20 (1984) 1021–1029.
Szabo Z., Rice D.E., Plummer L.N., Busenberg E., Drenkard S. and Schlosser P. (1996) Age-dating of shallow groundwater with chlorofluorocarbons, tritium/helium 3, and flow path analysis, southern New Jersey coastal plain. *Water Resour. Res.* **32(4)**, 1023-1038.
Tang, D.H., Frind, E.O., Sudicky, E.A., Contaminant transport in fractured porous media: Analytical solution for a single fracture, Water Resour. Res. 17 (1981) 555–564.
Therrien, R., Sudicky, E.A., Three-dimensional analysis of variably-saturated flow and solute transport in discretely-fractured porous media, J. Contam. Hydrol. 23 (1996) 1–44.
Thompson G.M. (1976) *Trichloromethane: A New Hydrologic Tool for Tracing and Dating Groundwater*. Ph.D. Dissertation, Department of Geology, Indiana University, Bloomington, Indiana. 93pp.
Thompson G.M. and Hayes J.M. (1979) Trichlorofluoromethane in groundwater: A possible tracer and indicator of groundwater age. *Water Resour. Res.* **15(3)**, 546-554.
Thompson G.M., Hayes J.M. and Davis S.N. (1974) Fluorocarbon tracers in hydrology. *Geophys. Res. Lett.* **1**, 177-180.
Tolstykhin, I.N., Kamensky, I.L., Determination of groundwater ages by the T-3He method, Geochem. Int. 6 (1969) 810-811.
Torgersen, T., Clarke, W.B., Jenkins, W.J., "The tritium/helium-3 method in hydrology", Isotope Hydrology 1978 (Proc. Symp. Neuherberg, 1978), vol. 2, IAEA, Vienna (1979) 917-930.
Tullborg, E.L., Gustafsson, E., 14C in bicarbonate and dissolved organics — a useful tracer? Appl. Geochem. 14 (1999) 927–938.
USGS 2018. Chlorofluorocarbons background. *Excerpt from Environmental Tracers in Subsurface Hydrology* Peter Cook and Andrew Herczeg(eds.) Kluwer Acadmic Press. https://water.usgs.gov/lab/chlorofluorocarbons/background/ Accessed December 2018.
Wassenaar, L.I., Aravena, R., Fritz, P., The geochemistry and evolution of natural organic solutes in groundwater, Radiocarbon 31 (1989) 865–876
Wassenaar, L.I., Aravena, R., Hendry, M.J., Fritz, P., Barker, J.F., Radiocarbon in dissolved organic carbon, a possible groundwater dating method: Case studies from western Canada, Water Resour. Res. 27 (1991) 1975–1986.
Wood, W.W. and Sanford, W.E., 1995. Chemical and Isotopic Method for Quantifying Ground-Water Recharge in a Regional, Semiarid Environment. Ground Water, 33(3): 458-486.
Love A.H. and A. Zdon, 2018. *Use of Radiocarbon Ages to Narrow Groundwater Recharge Estimates in the Southeastern Mojave Desert, USA, Hydrology MDPI*
Zdon, A., Davisson, M.L. and A. H. Love (2018) Understanding the source of water for selected springs within Mojave Trails National Monument, California, Environmental Forensics, 19:2, 99-111, DOI: 10.1080/15275922.2018.1448909

Appendix B: Photographs of Field Locations from this Study

Image taken from above spring orifice.

Evaporites at elevation higher than spring orifice

.

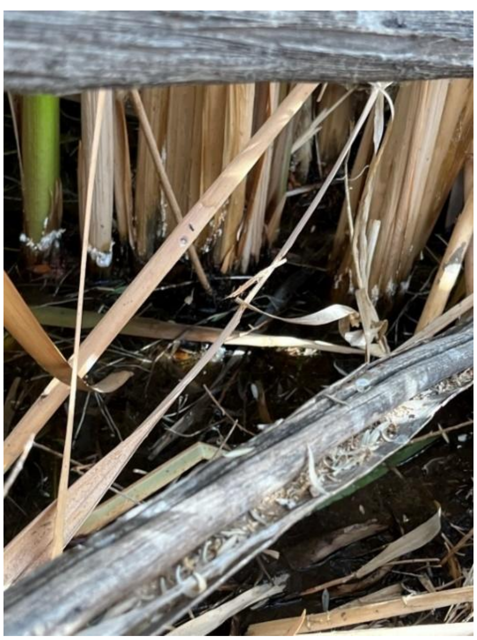

Water in the wash with Arundo donax.

Location of sample from the lower wash, next to the snake information sign.
(Dr. Dave Kreamer and student Collin Davidson in photo).

Flowing water in lower wash, below second sample point.

Looking downgradient to the south with Bonanza Spring toward lower Fenner watershed.

Bonanza Spring at the base of the Clipper Mountain looking north.

Bonanza Spring.

Field Water Quality sampling




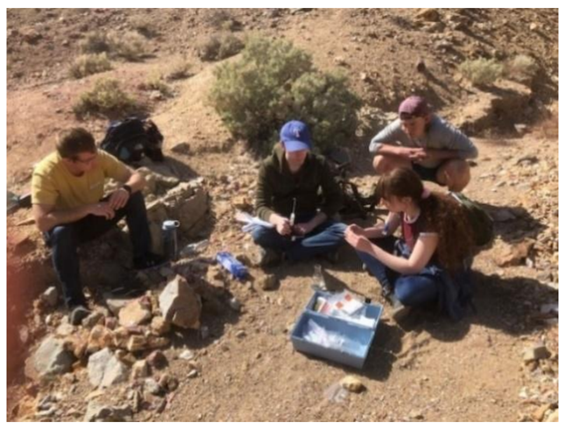
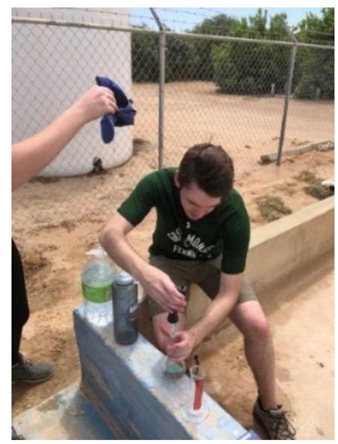

Left to right: Tyler Andres, Luke Stevens, Sandra Joseph, Collin Davidson



Appendix C: Principal Component Parameters

Table 1 Variance explained by Principal Components.

Importance of Components			
Component	Standard Deviation	Proportion of Variance	Cumulative Proportion
PC 1	3.872664	0.555464	0.555464
PC 2	2.659876	0.2620348	0.8174988
PC 3	2.025253	0.159129	0.9766278
PC 4	0.742452	0.02041611	0.99704391
PC 5	0.52407	0.0101722	1.000
PC 6	3.30E-15	4e-31	1.000

Table 2 Weightings of PC 1 and 2 by parameter used in the analysis.

Weightings of Principal Components 1, 2, and 3			
Parameter	PC1	PC2	PC3
As	-0.18432	-0.24579	0.087152
Ba	-0.21464	-0.01165	0.2548
Ca	0.161127	0.06135	-0.33885
Ce	-0.19985	0.053419	-0.30461
Dy	-0.23837	0.142367	0.019777
Er	-0.20866	0.219776	0.009739
Eu	-0.20832	0.202179	0.118208
Fe	-0.12221	0.211149	-0.32614
Gd	-0.24365	0.028563	0.142927
Ho	-0.20202	0.229691	0.045955
K	0.203127	0.210486	-0.1246
La	-0.21025	0.082002	-0.26545
Mg	0.199608	0.191764	-0.17474
Na	-0.17421	-0.27118	-0.03524
Nd	-0.2483	0.021187	-0.13042
Pb	-0.05899	0.141653	0.437254
Pr	-0.23636	0.12469	-0.11221
Sb	0.112731	0.265603	0.221642
Se	-0.18228	-0.25951	-0.0661
Sm	-0.25367	0.032939	0.067254
Tb	-0.20091	-0.18385	-0.18686
Th	-0.16359	0.171216	-0.29423
Tm	-0.15441	0.292104	0.085758
U	-0.1966	-0.19928	0.162515
Yb	-0.14898	0.302877	0.051674
dD	0.213573	0.130227	-0.01353
dO	-0.10397	-0.30332	-0.14776

Appendix D: Elemental Concentrations from ICP-MS

Table 3 Results of ICP-MS Analysis

Vial Label	Bonanza	Bonanza	Bonanza	Bonanza	Bonanza	Well 26	Well 33	Well 27s	Well 21N
Date	8/13/22	9/16/22	10/14/22	10/15/22	11/4/22	11/4/22	11/4/22	11/4/22	11/4/22
As			15.1	13.1	12.5	5.9165	7.8128	5.8942	5.1651
Ba			31.4	26.3	27.24	18.7844	31.6336	14.7298	11.6506
Ca			1966	1998	1666	2539	1584	2962	2760
Ce			BDL	BDL	0.021	0.030	0.007	0.009	0.010
Dy			BDL	BDL	0.003	0.005	0.004	BDL	BDL
Er			BDL	BDL	0.002	0.004	0.004	0.001	0.001
Eu			BDL	BDL	0.004	0.006	0.006	0.003	0.002
Fe	8.1162	8.1162	2.92	1.32	5.74	7.32	2.08	3.39	2.60
Gd			0.024	0.023	0.015	0.014	0.017	0.008	0.007
Ho			BDL	BDL	0.001	0.003	0.003	0.001	0.001
K			1236	1166	1609	6050	4303	6552	6251
La			0.018	0.018	0.014	0.018	0.007	0.006	0.007
Mg			1878	1536	1039	8486	4862	9618	9275
Na			200669	203514	129181	59992	68654	70234	64135
Nd	0.0469		0.021	0.022	0.014	0.015	0.006	BDL	BDL
Pb	0.0343		BDL	BDL	0.016	0.021	0.200	0.024	BDL

Vial Label	Bonanza	Bonanza	Bonanza	Bonanza	Bonanza	Well 26	Well 33	Well 27s	Well 21N
Date	8/13/22	9/16/22	10/14/22	10/15/22	11/4/22	11/4/22	11/4/22	11/4/22	11/4/22
Time	11:12	10:35	13:07	1:08	14:37	9:32	9:59	10:33	11:04
Pr	0.0134	BDL	0.009	0.009	0.005	0.008	0.005	0.003	0.003
Sb	177*	178.674*	0.342	0.307	0.88	2.00	2.80	2.57	1.49
Se		3.062715	2.54	1.81	BDL	BDL	BDL	BDL	BDL
Sm	0.0088	BDL	0.017	0.016	0.009	0.010	0.011	0.005	0.004
Tb	0.0012	BDL	0.541	0.549	0.251	0.160	BDL	0.052	0.052
Th	0.0071	BDL	0.026	0.026	BDL	0.086	BDL	BDL	BDL
Tm		BDL	BDL	BDL	0.001	0.003	0.003	0.001	0.001
U	3.40	3.41	2.27	2.11	1.39	0.98	1.44	0.95	0.76
Yb			BDL	BDL	0.002	0.004	0.004	0.001	0.001

Vial Label	Well 35	Bonanza	Bonanza	Bonanza DS	Alluvial Rattle	Bonanza	Bonanza	Well 35	Well 35
Date	11/4/22	12/30/22	12/30/22	12/30/22	12/30/22	1/28/23	1/28/23	1/28/23	1/28/23
As	7.7316	11.9969	12.1319	10.6434	17.0752	12.8092	11.9052	10.2130	10.8541
Ba	11.9140	29.5885	26.0332	26.6261	10.2633	35.4758	33.1971	16.8362	17.7571
Ca	2175	1930	1939	2027	2430	1699	1632	2296	2359
Ce	0.005	BDL	0.0658	0.0992	0.7105	0.0076	0.0102	BDL	BDL
Dy	BDL	BDL	0.0052	0.0062	0.0159	0.0043	0.0042	0.0027	0.0026
Er	0.001	BDL	0.0025	0.0027	0.0076	0.0036	0.0036	0.0030	0.0029
Eu	0.002	0.0034	0.0043	0.0047	0.0071	0.0064	0.0060	0.0047	0.0047
Fe	1.29	0.28	11.0	17.6	89.3	1.11	2.63	2.37	3.80
Gd	0.006	0.0128	0.0167	0.0195	0.0298	0.0187	0.0168	0.0094	0.0094
Ho	0.001	BDL	0.0011	0.0013	0.0031	0.0031	0.0030	0.0028	0.0028
K	5535	1831	2757	2022	2751	1420	1500	4948	5172
La	0.004	0.0045	0.0310	0.0499	0.1570	0.0107	0.0116	0.0057	0.0049
Mg	6983	1168	1288	1179	2627	942.8	862.2	6884	7125
Na	65742	159839	165284	159676	452033	118,257	118,254	58,552	58,435
Nd	BDL	0.0041	0.0295	0.0571	0.1274	0.0137	0.0146	0.0063	0.0054
Pb	0.016	BDL	0.0111	0.0251	0.0319	BDL	BDL	0.3444	0.3330

Vial Label	Well 35	Bonanza	Bonanza	Bonanza DS	Alluvial Rattle	Bonanza	Bonanza	Well 35	Well 35
Date	11/4/22	12/30/22	12/30/22	12/30/22	12/30/22	1/28/23	1/28/23	1/28/23	1/28/23
Time	11:39	10:37	10:38	9:03	9:00	1:32	1:34	11:19	10:25
Pr	0.002	BDL	0.0080	0.0151	0.0366	0.0046	0.0047	0.0029	0.0025
Sb	1.78	0.0868	0.0929	0.0993	1.1027	0.1826	0.1713	0.2931	0.2050
Se	BDL	1.45	1.10	0.1384	BDL	1.06	0.2302	3.07	3.50
Sm	0.004	0.0078	0.0120	0.0169	0.0263	0.0130	0.0125	0.0073	0.0071
Tb	BDL	BDL	0.7160	0.9769	2.65	0.4241	0.3676	BDL	0.0851
Th	BDL	0.0557	0.0290	0.0236	0.0377	BDL	BDL	0.0573	0.0255
Tm	0.001	0.0006	0.0007	0.0008	0.0013	0.0022	0.0022	0.0022	0.0022
U	1.21	1.74	1.61	1.55	1.06	2.51	2.41	2.24	2.30
Yb	0.001	0.0004	0.0015	0.0015	0.0058	0.0027	0.0028	0.0025	0.0026

Vial Label	Well 33	Well 21N	Well 21N
Date	1/28/23	1/28/23	1/28/23
Time	10:38	10:57	11:00
As	6.4536	5.9012	5.7434
Ba	33.8931	11.8487	11.3305
Ca	1580	2526	2607
Ce	BDL	BDL	0.0101
Dy	0.0025	0.0027	0.0027
Er	0.0028	0.0029	0.0030
Eu	0.0055	0.0038	0.0038
Fe	3.06	2.27	1.89
Gd	0.0140	0.0072	0.0069
Ho	0.0027	0.0027	0.0027
K	3933	6232	6168
La	0.0051	0.0072	0.0130
Mg	4712	8085	8339
Na	60,577	55,362	55,472
Nd	0.0053	0.0063	0.0096
Pb	0.6469	0.0388	0.0271
Pr	0.0023	0.0029	0.0038
Sb	0.2709	0.2269	0.1095
Se	0.1809	0.2195	0.2424
Sm	0.0107	0.0059	0.0056
Tb	BDL	0.0973	BDL
Th	BDL	BDL	BDL
Tm	BDL	BDL	BDL
U	2.58	1.65	1.67
Yb	BDL	BDL	BDL

*Large Sb values for Bonanza Spring measured in August and September 2022 are a result of molecular interferences not removed by the UNLV ICP-MS.

Appendix E: Stable Isotope Data

Table 4 Stable isotopes measured at Bonanza Spring and Cadiz Wells.

Site Name	Sample Date	Sample Time	Analysis Date	δD H_2O ‰	$\delta^{18}O$ H_2O ‰
Alluvial	12/30/2022	11:09	2/14/2023	-80.6	-9.97
Below Rattle Snake	12/30/2022	10:35	2/14/2023	-81.6	-10.07
Bonanza	2/26/2023	9:47	3/11/2023	-83.1	-10.57
Bonanza	1/28/2023	13:13	2/14/2023	-84.2	-10.64
Bonanza	11/4/2022	13:27	11/29/2022	-84.8	-10.67
Bonanza	10/15/2022	7:19	10/25/2022	-84.0	-10.61
Bonanza	10/15/2022	9:56	10/25/2022	-84.7	-10.74
Bonanza	10/14/2022	16:00	10/25/2022	-83.8	-10.66
Bonanza	10/14/2022	19:00	10/25/2022	-84.3	-10.66
Bonanza	10/14/2022	22:00	10/25/2022	-83.9	-10.63
Bonanza	10/15/2022	1:00	10/25/2022	-84.0	-10.65
Bonanza	10/15/2022	4:00	10/25/2022	-83.7	-10.62
Bonanza	9/2/2022	10:14	9/14/2022	-83.5	-10.61
Bonanza	8/13/2022	8:56	9/13/2022	-84.1	-10.61
Bonanza	7/21/2022	11:13	8/2/2022	-83.9	-10.64
Bonanza	3/13/2022	15:12	6/24/2022	-84.2	-10.59
Bonanza	12/30/2022	9:29	2/13/2023	-84.9	-10.67
Bonanza	12/30/2022	9:32	2/13/2023	-84.6	-10.63
Bonanza	12/30/2022	10:27	2/13/2023	-84.2	-10.64
Rattle Snake Sign	12/30/2022	10:35	2/14/2023	-72.6	-7.28
Rattle Snake Sign	3/13/2022	16:00	6/24/2022	-77.4	-9.1
Well 21N	11/4/2022	9:19	11/29/2022	-79.7	-10.74
Well 21N	10/14/2022	10:20	10/25/2022	-81.5	-10.95
Well 21N	8/13/2022	12:43	9/13/2022	-80.9	-10.82
Well 22	11/4/2022	10:00	11/29/2022	-80.5	-10.85
Well 23S	11/4/2022	10:21	11/29/2022	-80.1	-10.86
Well 24A	8/13/2022	12:18	9/13/2022	-81.2	-10.96
Well 26	1/28/2023	8:55	2/14/2023	-82.1	-11.06
Well 27S	11/4/2022	10:35	11/29/2022	-82.2	-11.06
Well 27S	1/28/2023	12:13	2/14/2023	-81.7	-10.98
Well 33	1/28/2023	10:45	2/14/2023	-82.7	-11.17
Well 33	11/4/2022	9:47	11/29/2022	-82.2	-11.10
Well 34	10/14/2022	11:15	10/25/2022	-81.6	-11.04
Well 35	11/4/2022	11:02	11/29/2022	-81.5	-11.01
Well 35	10/14/2022	11:44	10/25/2022	-81.2	-10.95

Notes on Site Names in Table 4

Alluvial Rattle – Sample taken from the first emergence from the alluvium, 3.05 m (10 ft) from the Rattle Snake information sign.

Bonanza DS – Taken at the cave opening at the start of the densely vegetated portion of the spring. Taken downstream from the orifice, which was about 6.1 m (20 ft higher) at the other opening of the cave. The upper cave opening has since collapsed.

Bonanza Spring – Bonanza samples taken on August 13th 2022 and September 16th 2022 were analyzed in the UNLV LVIS lab. Samples collected in August and September show high Sb concentrations. This is due to molecular interferences associated with the UNLV ICP-MS, and the values are not used in analysis. Blank cells in the table were not analyzed by the lab.

Appendix F: Additional Data

Table 5 Major Ion concentrations of sites.

Ion Chromatography Results (ppm)							
Vial Label	Fluoride	Chloride	Sulfate	Alkalinity	Calcium	Magnesium	Sodium
Well 34 10/14/2022 11:11	0.826	37.5	41.7	136	24.73	9.921	81.565
Well 35 10/14/2022 11:40	1.34	39.6	42.9	166	24.91	9.948	98.531
Bonanza Spring 10/14/2022 13:00	1.05	37.1	83.6	160	19.66	1.878	200.669
Bonanza LS 10/15/2022 1:28	1.08	37.2	83.8	188	19.98	1.536	203.514
Bonanza Spring 2/26/2023 9:53	1.07	37.16	65.14	199.5	14.12	0.870	114.990
Well 21N 4/29/2023 9:05	0.88	55.96	38.86	128.1	31.24	8.18	58.96
Well 26 4/29/2023 9:25	1.29	38.72	35.43	132.6	27.3	7.08	54.17
Well 27S 4/29/2023 10:03	1.26	38.5	35.86	128.5	25.21	6.21	56.22

Table 6 Results of total organic carbon (TOC), inorganic carbon (IC), and total nitrogen (TN) sampling.

TOC-TN Results	Concentration (ppm)			
Parameter	[TC]	[IC]	[TOC]	[TN]
BS 12/30/2022 9:44 TB	40.6	38.5	2.09	1.85
Site 1 1/28 9:48	26.46	25.70	0.76	3.88
Site 2 1/28 10:50	23.86	23.18	0.68	3.88
Site 3 1/28 LJS	26.17	26.36	0.00	3.42
BS 1/28/2023	39.02	38.52	0.50	1.25
Bonanza Spring 1 LJS 2/26/2023 9:32am 4	40.68	38.87	1.81	4.74
Bonanza Spring Alluvial LJS 2/26/2023 9:39am 5	35.43	32.83	2.6	15.48

Appendix E: R Code for PCA

```
# load necessary libraries
library(ggplot2)
library(factoextra)
library(ggcorrplot)
library(corrr)
library(ggfortify)
library(plot3D)
# Read CSV as dataframe. Verify is dataframe
excelData <- read.csv("PCA_Bonanza.csv")
class(excelData)

# Read CSV as dataframe, make date field null
bonanzaCorrData <- read.csv("BonanzaCorr.csv")
bonanzaCorrData$date <- NULL

rownames(excelData) <- excelData$Site.Name
excelData$Site.Name <- NULL

# Dataframe with loadings and PCs
pcaBonanza <- prcomp(excelData, retx = TRUE, center = TRUE, scale. = TRUE, tol = NUL
L)
components <- pcaBonanza[["x"]]
components <- data.frame(components)


# Making the covariance matrix
dataNormalized <- scale(excelData)
corrMatrix <- cor(dataNormalized)
corrplot(corrMatrix)

bonanzaDataNormalized <- scale(bonanzaCorrData)
bonanzaCorrMatrix <- cor(bonanzaDataNormalized)
corrplot(bonanzaCorrMatrix)

# Shows proportion of variance and cumulative variance
summary(pcaBonanza)

# Screeplot of variance
#screeplot(pcaBonanza,xlab = "Principal component")
autoplot(pcaBonanza,label = TRUE, label.size=3, loadings= TRUE,loadings.label = TRUE
, loadings.label.size = 3)

results <- pcaBonanza$x
# Suggests number of clusters to use
```

```
fviz_nbclust(results, FUNcluster = kmeans, k.max=5)
# Plots Kmean clusters
km1 <- eclust(pcaBonanza$x, "kmeans", hc_metric="manhattan",k=3)
#autoplot(kmeans(unlist(pcaBonanza), 3), data = pcaBonanza,label = TRUE, label.size=
3, loadings= TRUE,loadings.label = TRUE, loadings.label.size = 3)

pcaTransform = as.data.frame(-components[,1:3])
kmeansPCA = kmeans(pcaTransform,centers = 4, nstart=50)
fviz_cluster(kmeansPCA,data=pcaTransform)


fviz_pca_var(pcaBonanza, col.var="contrib", gradient.cols = c("#00AFBB", "#E7B800",
"#FC4E07"),repel = TRUE)
fviz_pca_biplot(pcaBonanza,axes=c(1,2),repel=TRUE)

varExplained = pcaBonanza$sdev^2/ sum(pcaBonanza$sdev^2)
qplot(c(1:6), varExplained) +
  geom_line() +
  xlab("Principal Component") +
  ylab("Variance Explained") +
  ggtitle("Scree Plot") +
  ylim(0,1)

plot3d(pcaPoints[,1:3], col=seq(nrow(pcaPoints)),size=8,repel=TRUE)
text3d(pcaPoints[,1:3],texts=(rownames(pcaPoints)))
```